Department of Companion Animals and Horses
University of Veterinary Medicine, Vienna

Clinical Unit of Diagnostic Imaging
(Head: Univ. Prof. Dr. med. vet. habil. Eberhard Ludewig (Dipl. ECVDI))

Assessment of Adrenal Computed Tomography Characteristics in Cats with Non-Adrenal Disease

Doctoral thesis submitted for the fulfilment of the requirements
for the degree of

DOCTOR MEDICINAE VETERINARIAE

University of Veterinary Medicine Vienna

Submitted by
Mag. med. vet. Stefanie Gaisbauer

Vienna, July 2021

First Supervisor: Univ. Prof. Dr. med. vet. habil. Eberhard Ludewig (Dipl. ECVDI)
Clinical Unit of Diagnostic Imaging
Department for Companion Animals and Horses
University of Veterinary Medicine, Vienna

Second Supervisor: Priv.-Doz. Dr. med. vet. Florian K. Zeugswetter
Clinical Unit of Internal Medicine of Small Animals
Department for Companion Animals and Horses
University of Veterinary Medicine, Vienna

Reviewer: Univ. Prof. Dr. med. vet. Iwan Burgener (Dipl. ECVIM-CA
Dipl. ACVIM PhD)
Clinical Unit of Internal Medicine of Small Animals
Department for Companion Animals and Horses
University of Veterinary Medicine, Vienna

Table of content

Dedication

To my partner, family, friends and to you the reader of this thesis.

1 Introduction and objective

With the increasing frequency and ever improving quality of computed tomography (CT), veterinary radiologists are more and more routinely evaluating feline adrenal glands on CT. Clear and accurate reference intervals are paramount for the distinction of pathological changes from normal adrenal morphological variance. References of adrenal gland characteristics have been provided in healthy cats for ultrasonography and CT and for cats with non-adrenal disease in ultrasonography (Cartee 1993, Zimmer 2000, Zatelli 2007, Combes 2013, Phoomvuthisarn 2018, Mallol 2019). To our knowledge adrenal computed tomography characteristics (aCTc) have until now not been evaluated for cats with non-adrenal disease. The already available studies serve as a baseline to distinguish normal morphology from pathology, however when it comes to evaluation of adrenal morphology in cases of non-adrenal disease there is a clear deficit. Studies about the prevalence and characteristics of feline adrenal masses in CT are also sparse and literature currently consists of a handful of case studies that describe the CT characteristics of adrenal masses in cats (Rijnberk 2001, Leshinsky 2016, Kirkwood 2019). In human medicine, adrenal masses are mostly detected incidentally with an incidence of 3–7% (Bovio 2006, Choyke 2006, Mayo-Smith 2017). In contrast, the incidence of incidental feline adrenal masses has not been determined. We suspect the incidence of these incidental masses is probably low, as the incidence of adrenal neoplasia in cats is only 0.03% (Myers 1997).

Our first objective was to describe aCTc in cats with no evidence of adrenal disease that underwent CT for non-adrenal disease (NAD-group). Our second objective was to determine the morphological deviations of aCTc in cats with possible concurrent adrenal disease (PAD-group) and to establish the prevalence and characteristics of adrenal masses in this selected cat population.

Intra- and inter-observer agreement of the parameter of aCTc were assessed to test the quality of the measurements. The conducted research resulted into a publication, which is the centrepiece of this doctoral thesis. The publication was accepted for publication on June 17th, 2021 by the Journal of the American Animal Hospital Association. The doctoral thesis gives a more in-depth insight into literature and adds complementary information, which was not possible in the limited setting of the publication.

2 Literature

2.1 Characteristics of the normal adrenal gland

The adrenal glands are paired endocrine glands, which have a cortex and a medulla. The cortex derives from the mesoderm and the medulla from the ectodermal primordium of the sympathetic nervous system (Koenig 2019). The cortex is divided into three layers (Figure 1). Superficial is the Zona glomerulosa, in the middle is the Zona fasciculata and central is the Zona reticularis (Ettinger 2010). The adrenal cortex produces three main types of steroid hormones: mineralocorticoids, glucocorticoids, and androgens. The activity of the adrenal cortex is regulated by the pituitary gland with adrenocorticotropic hormone (ACTH). The adrenal medulla produces adrenaline and noradrenaline (Koenig 2019).

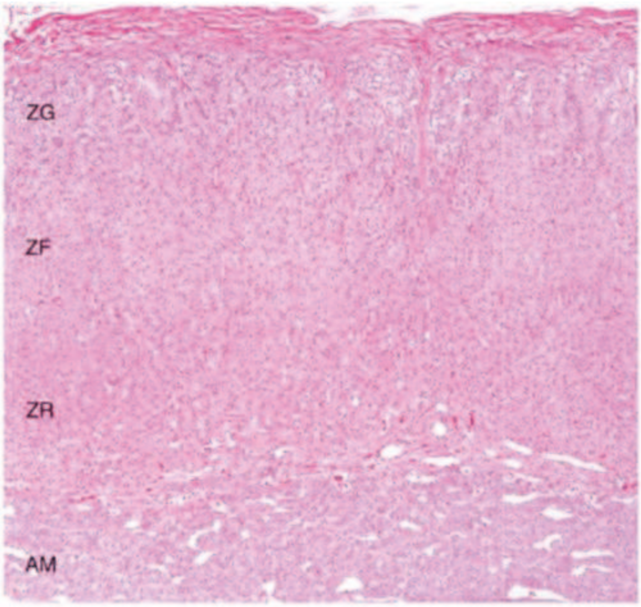

Figure 1 Histopathology of a normal adrenal gland showing the tree layers of the adrenal cortex (Ettinger 2010). Haematoxylin and eosin stain. AM = adrenal medulla, ZF = Zona fasciculata, ZG = Zona glomerulosa, ZR = Zona reticularis

Typically, adrenal glands of healthy cats are bipolar or oval and symmetric, less frequently they can be fusiform or wedge shaped and asymmetric (Cartee 1993, Zimmer 2000, Combes 2013, Phoomvuthisarn 2018, Mallol 2019). In comparison, ferrets show bilateral oval to oblong adrenal glands, whereas in dogs adrenal gland shapes are asymmetric. Their left adrenal gland is bilobed often referred to as “peanut” shaped and the right adrenal shape can vary but is usually wedge shaped (Barthez 1998, Nickel 2004, Kuijten 2007, Stieger-Vanegas 2018). Similarly, in humans, the adrenal glands are asymmetric. The right adrenal gland is pyramid-shaped and the left adrenal gland is more elongated, crescent shaped and regularly larger than the right adrenal gland (Schuenke 2018).

In cats, ferrets and dogs (Figure 2 and 3) adrenal glands are positioned retroperitoneal and in the craniomedial proximity of the cranial pole of the kidneys. In these species the left adrenal gland borders the Aorta abdominalis (Aabd) and the right adrenal gland borders the Vena cava caudalis (VCcd) (Koenig 1992, Barthez 1998, Nickel 2004, Kuijten 2007).

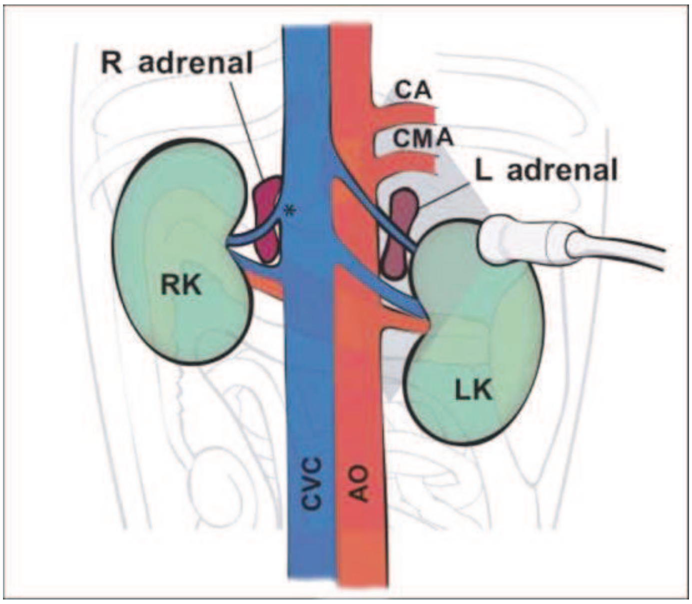

Figure 2 Schematic drawing of the position of the adrenal glands in a dog in dorsal recumbency (Penninck 2015).
AO = Aorta abdominalis, CA = Arteria coeliaca, CMA = Arteria mesenterica cranialis, CVC = Vena cava caudalis, R adrenal = right adrenal gland, RK = right kidney, L adrenal = left adrenal gland, LK = left kidney, * Vena phrenicoabdominalis

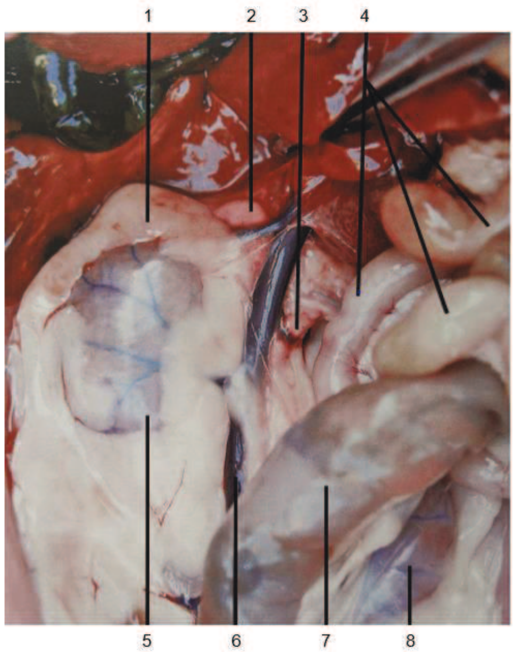

Figure 3 Abdominal situs showing the position of the adrenal glands of a cat in dorsal recumbency (adapted Koenig 2019).
1 = Capsula adipositas renalis, 2 = right adrenal gland, 3 = left adrenal gland, 4 = jejunum, 5 = right kidney, 6 = Vena cava caudalis, 7 = Colon descendens, 8 = left kidney

In dogs and cats the Vena phrenicoabdominalis and Arteria phrenicoabdominalis cross the adrenal glands ventrally, and dorsally, respectively (Koenig 1992, Barthez 1998, Nickel 2004). The human adrenal glands also lie retroperitoneal, but are attached to the cranial pole of the ipsilateral kidney. In agreement with the mentioned species the right adrenal of humans borders the Vena cava inferior. In contrast, the left adrenal does not border the Aabd in humans (Schuenke 2018).

In healthy cats, mean adrenal length is 10.3–11.4 mm and mean adrenal width or height 3.5–6.6 mm (Combes 2013, Phoomvuthisarn 2018, Mallol 2019). In ferrets, the range interval of adrenal size is even smaller with a mean adrenal length and width of 7.2–7.6 mm and 2.6–2.8 mm (O'Brien 1996). A widely varying adrenal size has been reported in different dog breeds. The maximum diameter (width/height) is 3–14 mm on the right and 3–16 mm on the left side. Length also varies widely with 10–39 mm and 10–50 mm on the right, respectively on the left side in healthy dogs or dogs with no clinical signs of endocrine disease (Barthez 1995, Grooters 1996, Douglass 1997, Hoerauf 1999). In humans, adrenal glands length measures up to 50 mm in normal adrenal glands of both sides. Diameter of the thin limb is 4–9 mm and of the wider body up to 10 mm (Slapa 2015).

The normal ultrasonographic findings of feline adrenal glands are described as a hypoechoic echogenicity surrounded by a thin hyperechoic halo of retroperitoneal fat and infrequently concentric layering with a more echoic centre can be seen. If this layering is equal to adrenal medulla and cortex is not known (Zimmer 2000, Combes 2013). In dogs, normal adrenal glands are also hypoechoic to the surrounding fat. Occasionally a thin hyperechoic line, which runs parallel to the capsule, may be seen. This line represents the intersection between cortex and medulla. Otherwise a more uniform hyperechoic medulla might be seen (Penninck 2015). Similarly, as in dogs and cats, adrenal glands are usually hypoechoic in humans, but an echogenicity which resembles that of the perirenal fat tissue is also possible. Corticomedullar differentiation is visible in human neonates, but it becomes indistinct with increasing age (Slapa 2015).

The attenuation of normal canine and feline adrenal glands in CT is homogenous and iso-dense to the kidney (Schwarz 2011). Mean adrenal attenuation in healthy cats is 32.1–35.5 Hounsfield Units (HU), which is similar in dogs with 34.3–36.0 HU (Schwarz 2011, Phoomvuthisarn 2018, Mallol 2019). Comparable to these, adrenal glands in humans also have a soft tissue attenuation of 25–40 HU (DeMaio 2011).

2.2 <u>Correlations of adrenal gland parameter with patient variables</u>

In cats the sex is not associated with adrenal size (Mallol 2019). Whereas in ferrets, bilateral adrenal width and right adrenal length was significantly larger in males. This could possibly be due to the significantly higher weight of male ferrets, as body weight correlated significantly with the width and length of the right adrenal gland (O'Brien 1996). In contrast, correlation of sex with adrenal size was inconsistent in dogs. No correlation was recorded by Douglass et al. (1997). However, Bento et al. (2016) registered a significantly larger adrenal thickness in males compared with females with a body mass >12–≤20 kg, and left adrenal thickness was larger in males than in females with a body mass >20–≤30 kg. In humans, study outcomes about a possible association also varied. In CT adrenal volume was not significantly different between the sexes, however in autopsies adrenal glands were significantly heavier in males (Lam 2001, Wang 2012).

In cats either a mild decrease of adrenal length with increasing age or no association of adrenal size with age has been reported (Combes 2012, Mallol 2019). Conversely a study in dogs found that adrenal thickness and body mass >12 kg were significantly positive correlated with age. For dogs with body mass ≤12 kg this was only true for left adrenal thickness (Bento 2016). Another sonographic study identified a significant positive correlation between dogs age and left adrenal gland length, but there was no significant correlation of age with right adrenal gland length or adrenal width (Douglass 1997). In humans, study results also varied. In one CT-study, adrenal gland volume did not change significantly with age, whereas in another study, there was a significant increase correlated with age (Meier 2007, Wang 2012).

In cats, body weight and body condition score (BCS) are not associated with adrenal size (Zatelli 2007, Mallol 2019). This is in contrast to dogs where a strong correlation of adrenal size with body weight was seen (Douglass 1997). Similarly, adrenal volume correlates significantly positive with body weight in humans (Wang 2012).

To our knowledge there are no CT-studies which examined the association of adrenal attenuation and delineation with signalment in dogs and cats. In adult humans a significant negative correlation of adrenal attenuation with age is seen (Meier 2007).

2.3 Adrenal mineralization

The mineralization in adrenals glands of cats is dystrophic (Herbach 2016). In general, dystrophic mineralization/calcification occurs in soft tissues undergoing apoptosis, necrosis, or fibrosis (Russell 1986, Kim 1995). In contrast with metastatic mineralization, it occurs although tissue fluid ion products of calcium and phosphate are within the physiological limits. Dystrophic mineralization is speculated to involve several mechanisms. The major mechanism of dystrophic mineralization probably is induced by damaged tissue, which exposes material with nucleating features to tissue fluids, which then induces mineralization. Isolated mitochondria, which are exposed to extracellular fluid can be initial sites of calcium phosphate deposition (Russell 1986).

As in humans, adrenal mineralization is a degenerative change in cats and it was positively correlated with age in a histopathological study. In the initial phase of mineralization, fine granular intracellular deposits neighboring apoptotic or necrotic cells were identified in feline adrenal glands. These deposits resemble cholesterol crystals and were clearly associated with adrenal mineralization. It was also assumed that they precede adrenal mineralization. There was a significant correlation of cortical adrenal mineralization with cell death in this study, but it was rarely linked to overt adrenalitis in cats (Herbach 2016).

Adrenal mineralization is a normal morphological variant in cats and a non-specific lesion in dogs and humans (Besso 1997, Hoenig 2002, Hindmann 2005). In cats it was present in histopathological analysis of 38% of cats and even in kittens younger than 6 months (Hoenig 2002, Herbach 2016). It is not indicative for adrenal neoplasia and in agreement with this, a literature search for this study resulted in only two cases of feline adrenal neoplasia that had adrenal mineralizations. In both cases, cortical adenocarcinoma was diagnosed (Becker 1999, Rossmeisl 2000, Hoenig 2002). Literature about adrenal mineralization associated with benign pathological adrenal changes detected in veterinary medical imaging was rare. The literature search resulted in only one case that reported hyperadrenocorticism combined with adrenal mineralization (Combes 2013).

In contrast, in a study about ultrasonographic visualization of adrenal glands in ferrets, no adrenal mineralizations were detected in 21 examined healthy ferrets. In only two (3%) adrenal glands of the 37 ferrets with clinical signs of hyperadrenocorticism mineralization was seen (Kuijten 2007).

In comparison, canine adrenal mineralization was seen in 7% of histopathological analysed adrenal glands. In dogs it was reported as a dystrophic change and was observed in adrenal vessels and capsules and occurrence increased significantly with age (Herbach 2016). Adrenal mineralization is non-specific in dogs (Besso 1997). It can occur in various adrenal tumours including pheochromocytoma, carcinomas, adenomas, but was also seen with morphological changes such as adrenal hyperplasia (Penninck 1988, Besso 1997, Maher 1997, Barthez 1998, Pey 2014).

In contrast to dogs and ferrets, but in agreement with cats, adrenal mineralization is common in humans (Hoenig 2002, Hindman 2005, Heinz-Peer 2007, Kuijten 2007, Herbach 2016). Although mineralization is non-specific in humans, the presence and pattern of adrenal mineralization can help to focus the differential diagnoses, when it is combined with other imaging features and the history of the patient (Hindman 2005, Elsayes 2017). Adrenal mineralization can be present in various adrenal lesions of humans (Hindmann 2005, Elsayes 2017). It occurs in malignant or benign neoplasia such as: neuroblastoma, myelolipoma, adenoma, haemangioma, adrenal mature teratoma, pheochromocytoma and adrenocortical carcinoma (Bravo 1984, Rofsky 1989, Newhouse 1999, Khong 2002, Rha 2003, Hindmann 2005, Else 2014). Frequency of mineralization can vary widely depending on tumour type from less than 10% in pheochromocytomas up to 85% in neuroblastomas in CT (Bravo 1984, Rha 2003). Primary neoplasms with a tendency to mineralizations include mucinous adenocarcinoma, osteosarcoma and papillary thyroid carcinoma. These can cause adrenal mineralization, when they metastasize to adrenal glands (Hindman 2005). Furthermore, adrenal mineralization was also seen in association with adrenal haemorrhage and subsequent haemorrhagic degeneration, (pseudo)cysts, abscesses, granulomatous disease (tuberculosis), histoplasmosis and the seldom lysosomal acid lipase deficiency (Wang 2003, Hindmann 2005, Hoffman 2015, Bouknani 2018, Ali 2019, Porntharukchareon 2019).

2.4 Influence of endocrine and non-adrenal neoplastic diseases on adrenal morphology

Although this topic is already mentioned in the discussion of the publication, we want to address it here in more detail. Various pathologies, especially endocrine diseases or neoplasia (functional or non-functional), can influence the morphology of adrenal glands (Watson 1998, Labelle 2005, Combes 2012, Lunn 2013, Lourenco 2015, Herbach 2016).

In cats with feline interstitial cystitis (FIC) a reduced cortisol response to synthetic adrenocorticotropic hormone was observed. Additionally, post-mortem adrenal gland volume was found to be significantly smaller in cats with FIC in comparison with healthy cats. These results suggest that cats with FIC may have a mild primary adrenal insufficiency as a co-morbidity (Westropp 2003).

Bilateral atrophy of adrenal glands has been reported in cats (on autopsy), dogs (on ultrasonography), and humans (on CT) with hypoadrenocorticism (Peterson 1989, Hoerauf 1999, Korobkin 1995). Still, there is no description of ultrasonographic abnormal findings in cats with hypoadrenocorticism (Combes 2014a, Woolcock 2015). We also did not identify any further imaging studies reporting reduced or changed adrenal size in cats with hypoadrenocorticism. More research is needed to assess the exact impact of adrenal atrophy on adrenal size measured with ultrasonography and CT in cats.

Pituitary functional neoplasms secreting ACTH or growth hormone cause pituitary hyperadrenocorticism and are the main cause of hypersomatotropism (acromegaly) in cats and humans (Lunn 2013, Dineen 2017). Pituitary hyperadrenocorticism can lead to bilateral adrenal enlargement due to cortical hyperplasia in cats, dogs, and humans (Grooters 1996, Watson 1998, Agrons 2017). Similarly, hypersomatotropism in cats and humans leads to bilateral adrenal enlargement (Pappa 2012, Lourenco 2015).

Furthermore, sonographic size of adrenal glands in cats with hyperthyroidism was significantly larger compared with healthy cats (Combes 2012). Hypersecretion of the adrenal glands seen in humans and cats with hyperthyroidism is suspected to be the cause of significant enlargement of the adrenal cortex (Gallagher 1972, Feldmann 2004a).

In cats, primary hyperaldosteronism caused by micronodular hyperplasia of the adrenal cortex can also cause a mild unilateral or bilateral thickening and rounding of adrenal glands seen in ultrasonography or CT (Javadi 2005).

2.5 Adrenal Neoplasia

Functional primary adrenal neoplasia in cats can cause hyperadrenocorticism, hyperaldosteronism and overproduction of sex hormones (Hoenig 2002, Feldman 2004b, Ash 2005, Briscoe 2009, Valentin 2014). Although these diseases have been described in cats, they are considered rare (Feldman 2004b, Combes 2014a, Valentin 2014). Myers (1997) searched the veterinary medical database over the period from 1985–1996 to determine the relative incidence of adrenal neoplasia in dogs and cats. He identified a very low incidence of adrenal neoplasia of 0.03% in cats and an incidence of 0.17% in dogs. Functionality of the neoplasias was not determined. In this same search Myers (1997) found 49 feline adrenal neoplasms. Fifty-six per cent (26 of 49) were primary neoplasias, for 28% (14 of 49) complete histopathological classification was not possible and 18% (9 of 49) were metastatic. Of the primary neoplasias, 69% (18 of 26) were cortical adenomas, 23% (6 of 26) cortical carcinomas, and 8% (2 of 26) pheochromocytomas or other neuroendocrine tumours. In this study, 934 canine adrenal tumours were diagnosed. Of those 70% (652 of 934) were primary neoplasias, 28% (258 of 934) were not classified, and 3% (24 of 934) were metastatic. Of the primary canine neoplasias, 58% (379 of 652) were adrenal cortical adenomas, 20% (129 of 652) cortical carcinomas, and 22% pheochromocytomas or other neuroendocrine neoplasia. In another study, most feline and canine adrenal masses were determined to be metastatic instead of primary neoplasia (Herbach 2016). This is in contrast with humans where adenomas are the most frequent adrenal neoplasia (Mansmann 2004). In cats, adrenal metastases are most frequently caused by lymphoma and less frequent by carcinomas, which is the reverse in dogs (Herbach 2016). In dogs metastases of melanomas to the adrenal glands were also reported (Labelle 2005).

Masses which are detected incidentally during medical imaging, surgery or clinical examination are called “incidentalomas”. In dogs incidentalomas were identified in 4–9% of ultrasonography or CT-examinations of the abdomen (Cook 2014, Baum 2016). A study that examined the prevalence of canine incidentalomas in ultrasonography reported 30% of the adrenal masses analysed with histopathology as malignant. Histopathologic diagnoses of the malignant incidentalomas included only cortical pheochromocytoma and cortical carcinoma, which occurred similarly frequent. All benign incidentalomas were adenomas (Cook 2014). In comparison to the many studies in human medicine about adrenal incidentalomas, these are scarce in veterinary medicine. To the best of our knowledge the incidence of adrenal incidentalomas is currently not known in cats.

In humans, most adrenal masses are detected incidentally when undergoing imaging for other reasons (Mansmann 2004, Elsayes 2017). The occurrence of incidentalomas in human adults in various studies was 3–7% (Bovio 2006, Choyke 2006, Mayo-Smith 2017). Most of these are benign non-hyperfunctional adenomas (Mansmann 2004). In autopsies, adrenal adenomas have a reported occurrence from 1.5%–32% (Kloos 1995). In patients that had incidentalomas on medical imaging or in surgery, 69–85% were non-functional, 9.2–12% secreted cortisol, 4.2–10% were pheochromocytomas, 8–11% were cortical adenocarcinomas, 0–7% were metastases and 1.6–6% were aldosteronomas (Kloos 1995, Mantero 2000, Fassnacht 2016). Metastases are the most common cause for malignant lesions of the adrenal gland in humans (Elsayes 2017, Mayo-Smith 2017). These metastases frequently originate from primary tumours of the lung, kidney, breast, pancreas, and gastrointestinal tract (Lee 1998). In contrast, primary adrenal tumours including pheochromocytomas, aldosteronomas, and cortical adrenocarcinomas are a very rare cause for adrenal neoplasia (Mayo-Smith 2017). The incidence of primary adrenal neoplasia is only seven cases per one million persons/year (0.0007%) in humans (Chandrasekar 2019).

2.6 Ultrasonography of adrenal neoplasia

Due to the rareness of adrenal neoplasia in cats, there are limited studies about their sonographic characteristics. In cats it is currently not possible to diagnose adrenal malign or benign disease based on sonographic adrenal characteristics alone. It is used as a complementary diagnostic tool to endocrine clinical and laboratory work up. In cats, it is considered a valuable routine screening tool to detect adrenal asymmetries caused by functional or non-functional primary adrenal neoplasia or metastases. A sonographic normal contralateral adrenal gland does not exclude bilateral infiltration and bilateral enlargement can be seen caused by pituitary hyperadrenocorticism, but also by adrenal neoplasia (Combes 2014a). Another rare cause of bilateral adrenal enlargement is bilateral adrenal neoplasia of differing aetiology (pheochromocytoma and adrenocortical adenoma) (Calsyn 2010). Differential diagnoses for bilateral sonographic adrenal enlargement or thickening not caused by adrenal neoplasia are: hyperthyroidism, hypersomatotropism and hyperaldosteronism caused by micronodular hyperplasia (bilateral or unilateral) (Javadi 2005, Combes 2012, Lourenco 2015).

As a diagnostic tool for adrenal lesions, ultrasonography has a low sensitivity in dogs with 63.7%, but specificity is considered good at 100% (Pagani 2016). In dogs with an adrenal lesion, a larger adrenal size has been proven to be associated with malignancy. In two studies, all adrenal masses over 20 mm diameter were malignant (Cook 2014, Pagani 2016). Research which compared adrenal lesions seen in ultrasonography to histopathological findings showed that all masses with vascular infiltrations in dogs were caused by malignant neoplasia (adrenocortical carcinoma, pheochromocytoma). In dogs, a nodular sonographic structure of the cortex was seen with cortical hyperplasia as well as with adrenocortical carcinoma and pheochromocytoma. (Pagani 2016).

In contrast with cats and dogs, abdominal ultrasonography is seldomly applied for examinations of adrenal glands in humans. It is only the modality of choice for imaging of adrenal pathologies in children or pregnant women to avoid ionising radiation from CT. Otherwise CT is the modality of choice for adrenal imaging in humans (Blake 2009a).

In veterinary medicine, new imaging methods are being introduced to improve sonographic examinations of the adrenal glands. Benign and malignant adrenal masses show significantly different characteristics in contrast enhanced ultrasonography (CEUS) (Pey 2014, Bargellini 2016). When enhancement degree and vascularity were combined, it was possible to differentiate benign and malignant adrenal lesions with a sensitivity of 100%, a specificity of 80%, and an accuracy of 92% (Bargellini 2016). Although Dietrich et al. 2010 concluded that CEUS could not differentiate adrenal malignant lesions from benign lesions in humans, the study from Friedrich-Rust et al. 2008 came to a different conclusion. A size >4 cm, hypervascularization, and early arterial or arterial contrast enhancement and rapid washout were significantly more often seen in malign than in benign lesions. In this study sensitivity (100%) and specificity (82%) of CEUS to diagnose malignant adrenal masses was comparable to that of CT and MRI.

2.7 <u>Computed tomography of adrenal neoplasia</u>

In small animals, ultrasonography rather than CT is more commonly used as the first imaging modality to examine the adrenal glands. Ultrasonography is non-invasive, but diagnostic quality is operator dependent and patient confirmation and bowel gas can hinder the examination (Tidwell 1997). The application of CT to diagnose morphological changes of abdominal organs is increasing in veterinary medicine. In human medicine, CT is the modality of choice (Blake 2009b). To evaluate the CT characteristics of adrenal lesions, it is important to include lesion size, homogeneity, presence of fat, hemorrhage, mineralization, attenuation on unenhanced and enhanced CT studies (Blake 2009b). To our knowledge, the literature regarding feline adrenal neoplasia examined with CT is currently limited to case studies (Rijnberk 2001, Leshinsky 2016, Kirkwood 2019). Literature about non-neoplastic diseases with influences on feline aCTc is also very limited. Still, these diseases should be considered as differential diagnoses for adrenal enlargement caused by uni- or bilateral adrenal neoplasia. Although bilateral adrenal enlargement was reported in sonographic examinations of cats with hyperthyroidism and hypersomatotropism, to our knowledge it has not been documented with CT (Combes 2012, Lourenco 2015). In contrast, mild uni- or bilateral adrenal thickening was reported in ultrasonography- and CT-studies in cats with hyperaldosteronism caused by micronodular hyperplasia of the adrenal cortex (Javadi 2005).

The literature regarding CT characteristics of adrenal neoplasias in dogs is more extensive, but remains limited especially when compared with human medicine. CT characteristics of primary adrenal neoplasia in 17 dogs were compared to histopathological diagnosis and characteristics at surgery or necropsy and their associations to tumour types were tested. Adenocarcinomas, pheochromocytomas and adenomas were diagnosed. Signs of vascular invasion seen on CT and seen at surgery or necropsy showed excellent agreement. This adrenal characteristic was the only one that showed significant association with pheochromocytomas. Furthermore, no other adrenal characteristic was significantly associated with any of the three diagnosed adrenal neoplasia types. The overlap of the characteristics of the different tumour types prohibited a reliable diagnosis based on CT. In general, the histological examination and the delayed post contrast CT images showed a significant association of a heterogenous pattern of enhancement of contrast with haemorrhage and/or infarction and between a contrast enhancing rim and a fibrous capsule of the tumour (Gregori 2015). A different study conducted triple-phase (native, arterial, venous, delayed phase) helical CT-scan to evaluate morphological adrenal characteristics in dogs. It also included CT values and calculations as percentage enhancement wash-in and percentage enhancement wash-out (see equation below). In this study it was feasible to diagnose different canine adrenal tumour types (adenocarcinomas, pheochromocytomas, adenoma) based on all these characteristics (Yoshida 2016).

In contrast to feline and canine medicine, there are plenty studies about CT characteristics of adrenal neoplasia in human medicine. In humans most incidentalomas are benign non-hyperfunctionial adenomas (Mansmann 2004). Therefore, the most important and first step in medical imaging is to differentiate between these adenomas and other masses (Elsayes 2017). At the start of diagnostic work up a non-enhanced CT including measurement of attenuation needs to be conducted. An attenuation value of <10 HU is typical for lipid rich adenomas and no further diagnostic imaging is recommended if this is the case (Caoili 2002). Of adenomas 10–40% are lipid-poor and it is not possible to distinguish them from other neoplasias (metastases, primary adrenocortical carcinoma, most pheochromocytomas) with non-enhanced CT (Blake 2009b). For adrenal masses with an attenuation of >10 HU additionally contrast enhanced CT imaging 60 seconds after intravenous contrast administration and a delayed scan after 15 minutes is advised.

After measuring the attenuation of the adrenal lesion in the enhanced and non-enhanced scans absolute or relative percentage of enhancement is calculated using the following equations (Caoili 2002).

$$\text{absolute \% enhancement washout} = \frac{\text{attenuation enhanced CT} - \text{attenuation delayed enhanced CT}}{\text{attenuation enhanced CT - attenuation unenhanced CT}} \cdot 100$$

$$\text{relative \% enhancement washout} = \frac{\text{attenuation enhanced CT} - \text{attenuation delayed enhanced CT}}{\text{attenuation enhanced CT}} \cdot 100$$

An absolute washout of >60% and a relative wash out of >40% was proved as highly sensitive (88%–96%) and highly specific (96%–100%) for diagnosing adrenal adenomas. (Caoili 2000, Caoili 2002, Park 2007).

Malignant lesions of the adrenal gland are most frequently caused by metastases in humans (Elsayes 2017, Mayo-Smith 2017). These occur bilaterally in almost half (49%) of the patients and more often on the left if unilateral (Lam 2002). The attenuation of metastases is usually >10 HU on native CT and they do not show significant enhancement washout on delayed phase. The absolute enhancement washout of metastases most frequently is <60% and relative enhancement washout <40% (Caoili 2002, Blake 2006, Elsayes 2017). In most patients differentiation of benign versus malignant adrenal masses is possible using contrast enhanced CT and calculation of wash out (Blake 2009b). On routine contrast enhanced CT, characteristics of adrenal metastases can be non-specific. An irregular margin or a broad enhancing rim is considered a characteristic of malignancy, conversely smooth margins and homogenous attenuation occur both in metastases and benign masses. In patients without a known history of cancer, malignant adrenal metastases are very rare (Song 2013). Primary adrenal tumours are also very rare in humans. The primary adrenal malignancies can be adrenocortical carcinoma, pheochromocytoma/paraganglioma, neuroblastoma, non-Hodgkin lymphoma and sarcoma, but also several other tumour types can occur in the adrenal gland (Mayo-Smith 2017, Elsayes 2017, Chandrasekar 2019). Some of these have typical characteristics, but they can also have non-specific characteristics or the characteristics overlap with those of other benign adrenal masses, which prevents an exact diagnosis on routine (enhanced) CT alone (Blake 2009b, Elsayes 2017). Further work up such as magnetic resonance imaging, biopsies, surgical resection or clinical follow up is needed. Diagnostic imaging is a useful way to distinguish benign from malign adrenal masses, but cannot assess if a mass is functional or non-functional. Therefore, clinical and laboratory work up is necessary (Blake 2009b).

3 Animals, material, and methods

For all patients of the NAD-group a full clinical history, complete physical examination including BCS and systolic blood pressure measurement, complete blood count, extensive plasma biochemistry profile including electrolytes, total thyroxine concentration (if ≥6 years of age), and urinalysis (including dips stick, sediment, and if indicated bacterial culture) was conducted. Table 1 shows the examined parameter and reference intervals of the plasma biochemistry and electrolytes which were used.

Table 1 Reference intervals and cut offs of laboratory blood and urine parameter

Blood parameter	Reference interval	Unit
ALT	<100	U/L
Albumin	2.6–4.6	g/dL
Total protein	6–7.5	g/dL
Creatinine	<1.6	mg/dL
BUN	20–65	mg/dL
Fructosamine	<340	µmol/L
Glucose	55–100	mg/dL
Sodium	142–164	mmol/L
Chlorine	111–130	mmol/L
Potassium	3.5–5	mmol/L
Phosphorous	0.8–1.6	mmol/L
Calcium	2–3	mmol/L
T4	19.00–45.57	nmol/L
Urine parameter		
Specific gravity	1.020–1.040	g/ml
pH	5–7	–
UPC	<0.33	–
UCC	8–42 x 10^6	–
Protein	2–63	mg/dL

ALT = alanine aminotransverase, BUN = blood urea nitrogen, T4 = total thyroxine concentration, UPC = urine protein:creatinine ratio, UCC = urine cortisol:creatinine ratio

All these examinations were performed to exclude diseases with possible influence on adrenal morphology (FIC, chronic kidney disease, hyperadrenocorticism, hypoadrenocorticism, diabetes mellitus, hyperthyroidism, primary hyperaldosteronism, hypersomatotropism, abnormal sexual hormone production, severe hypertension, adrenal neoplasia). If laboratory parameters exceeded the reference intervals, all other findings and laboratory parameters were precisely evaluated to decide whether to exclude this patient. In cases of doubt, an internal medicine specialist was consulted. Further work up of non-adrenal diseases was initiated as indicated and to the discretion of the university clinician in charge.

In NAD-group the systolic blood pressure was measured five times in series with a doppler ultrasonic flow detector (Model 811-B, Eickemeyer, Parks Medicals Electronics), sphygmomanometer and neonate disposable blood pressure cuffs (Philips, size one: 3.1–5.7 cm; size two: 4.3–8.0 cm; size three: 5.8–10.9 cm). The measurement was conducted prior to clinical examination and anaesthesia. The cuffs size was selected in a width of 30–40% of the circumference of the tail or forelimb. If any measurement was ≥ 179 mmHg the cat was excluded from the study to exclude severe systolic hypertension (Acierno 2018).

4 Publikation

Assessment of Adrenal Computed Tomography Characteristics in Cats with Non-Adrenal Disease

Stefanie Gaisbauer[1], Florian K Zeugswetter[2], Alexander Tichy[3], Conor Rowan[1], Eberhard Ludewig[1]

[1]Clinical Unit of Diagnostic Imaging

[2]Clinical Unit of Internal Medicine of Small Animals

[3]Platform for Bioinformatics and Biostatistics

University of Veterinary Medicine Vienna

Veterinaerplatz 1

1210 Vienna, Austria

Abstract

Reference intervals of adrenal CT characteristics (aCTc) in healthy cats are well known, but intervals for diseased cats are lacking. ACTc of cats with no evidence of adrenal disease (NAD-group) were compared to parameters of cats with possible concurrent adrenal disease (PAD-group). The PAD-group was assessed for adrenal masses or other morphological deviations using the NAD-group as reference. Associations of aCTc with patient variables were explored and additionally all results were compared with published aCTc of healthy cats.

No incidental adrenal masses were identified in the PAD-group (n=92) and only few aCTc differed when compared to the NAD-group (n=30). The NAD-group showed similar associations of patient variables and similar aCTc as length (right: 11.5 ± 2.2 mm, left: 11.8 ± 1.7 mm), width (right: 6.4 ± 1.2 mm, left: 5.4 ± 0.8 mm), height (right: 4.5 ± 0.9 mm, left: 4.5 ± 0.8 mm), attenuation (right: 33.1 ± 5.0 HU, left: 32.5 ± 5.3 HU) and position, but markedly more mineralization (right: 10 %, left 13.3 %) than reported in current literature involving healthy cats. This study provides references of aCTc for diseased cats without evidence of adrenal disease. The results suggest that adrenal incidentalomas seem rare in this population.

Introduction

Advanced diagnostic imaging, especially CT, is increasingly used to identify morphological changes of abdominal organs including the adrenal glands in cats. Accurate reference intervals and awareness of normal variants of adrenal glands facilitate the discrimination of adrenal disease from normal morphology.

Several ultrasonographic studies have described the adrenal characteristics of healthy and diseased cats with non-adrenal or adrenal disease.[1–4] Two recent studies investigated adrenal CT characteristics (aCTc) in healthy cats, but examinations including a group of diseased cats are lacking.[5,6] In cats with non-adrenal diseases references intervals of aCTc are not yet known and the prevalence of anatomic variants and pathological changes still needs to be determined. CT studies about adrenal disease in cats are currently limited to case reports about adrenal neoplastic masses.[7–9] With an incidence of 0.03 %, feline adrenal neoplasia is rare and unlike in humans and dogs, the prevalence of feline adrenal incidental masses is not known.[10–14]

Our objectives were to (1) describe aCTc in cats with no evidence of adrenal disease that underwent CT for non-adrenal disease (NAD-group) and (2) determine the prevalence of adrenal masses as well as to evaluate other morphological deviations of aCTc in cats with possible concurrent adrenal disease (PAD-group), using the NAD-group as a reference. Additionally, we aimed to compare all results with previously published adrenal gland variables in healthy cats.

Materials and methods

The study was set up as an observational study including one prospectively (NAD-group) and one retrospectively selected (PAD-group) study group.

NAD-group: Prospective study (cats with no evidence of adrenal disease)

Data for the NAD-group were collected in the period from October 2018 until July 2019. Recruitment of this group was done by asking clients of the Clinical Unit of Diagnostic Imaging, with cats meeting the inclusion criteria, to participate in the study. A written owner informed consent was obtained for all cats participating in the study. Inclusion criteria consisted of: age ≥1 year and presence of non-adrenal disease that warranted CT examination. A full clinical history, complete physical examination, complete blood count, extensive plasma biochemistry profile including electrolytes, total thyroxine concentration (if ≥6 years of age) and urinalysis was performed in each cat. A body condition score (BCS) of 1 (thin) to 5 (obese) according to Shoveller and others was applied.[15] Systolic blood pressure was determined to exclude patients with severe systolic hypertension (≥179 mm Hg).[16]

Exclusion criteria included the administration of drugs and diseases that could influence adrenal gland morphology. Specifically, cats treated with corticosteroids, spironolactone or an angiotensin converting enzyme inhibitor were excluded. Further, animals that underwent administration of iodinated contrast media within the last ten days prior the study as well as cats with suspected or confirmed diagnosis of the following conditions were excluded: feline idiopathic cystitis, chronic kidney disease, hyperadrenocorticism, hypoadrenocorticism, diabetes mellitus, hyperthyroidism, primary hyperaldosteronism, hypersomatotropism, abnormal sexual hormone production, severe hypertension and adrenal neoplasia. Presence of non-adrenal diseases that were unlikely to impact adrenal function or adrenal mineralisation did not warrant exclusion. The remaining cats were considered to have normal adrenal gland structure and function and were thus included.

PAD-group: Retrospective study (cats with possible adrenal disease)

The archive of the Clinical Unit of Diagnostic Imaging of the University of Veterinary Medicine Vienna was searched for all CT studies of cats that included the adrenal gland region (June 2009 to September 2018). A slice thickness $\leq$ 1 mm, a quality of the CT scan which ensured unrestricted adrenal assessment and a patient age of $\geq$1 year was required for inclusion. Unlike the NAD-group, all cats were included regardless of underlying disease process, including diseases that may alter adrenal morphology. Patients that had received iodinated contrast media within the last 10 days prior to the study or with signs of incomplete contrast media excretion were excluded.

Data collected from medical records included: age, breed, sex, body weight, BCS, indication for CT, CT acquisition parameters and body position during CT.

All procedures in this study were approved by the institutional ethics and animal welfare committee of the University of Veterinary Medicine Vienna in accordance with good scientific practice guidelines and national legislation (ETK-09/07/2018 - number of ethical committee for approval).

<u>Image analysis</u>

Images were analysed by one radiologist (SG), using a dedicated workstation and the imaging software JiveX Diagnostic Advanced 5.0.4.4[a]. Adrenal measurements were conducted using soft tissue window settings (window level: +350 Hounsfield Units [HU], window width: +40 HU). Delineation was graded as: very good (0), good (1), moderate (2), poor (3). All adrenal dimensions were measured with a digital caliper in two planes and the larger measurement was recorded. Length was measured from the cranial to the caudal borders, width from the medial to the lateral borders and height from the ventral to the dorsal borders, all at the level of maximal dimension (Figure 1A, B). Adrenal glands were categorized into one of three commonly recognized shape patterns: bipolar (oval with a depression over the minor axis), oval (without depression) or arrowhead (wedge shape with rounded caudal tip) (Figure 2A, B). Adrenal gland attenuation was measured in HU by placing a region of interest (ROI) outline over the largest cross-sectional area of the adrenal gland in the sagittal or dorsal plane (Figure 3A). The ROI outline was traced by hand. The phrenicoabdominal vessels and the adrenal gland borders were excluded to avoid partial volume effects and exclude periadrenal fat. The adrenal position relative to major vasculature, bordering vessels/organs, presence of adrenal mineralization (Figure 3B) or masses was noted.

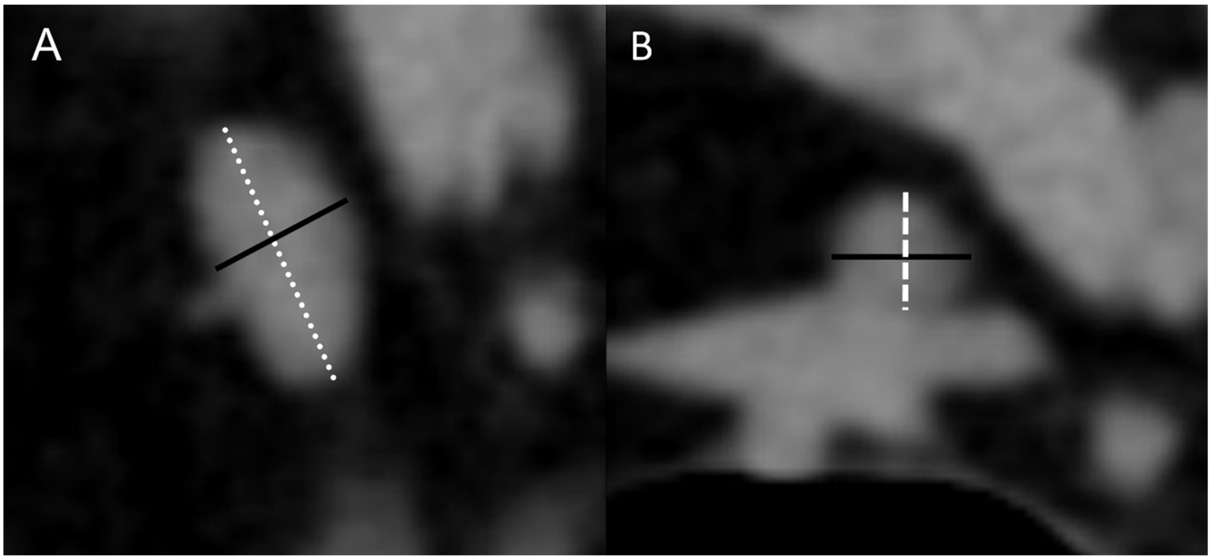

Figure 1 Dorsal (A) and transverse (B) CT image of an oval right adrenal gland of a cat displayed in soft tissue window. All distances for adrenal gland size were measured with a digital caliper in both planes. The maximal dimension was recorded: length - dotted white line, width - solid black line, height - discontinuous white line.

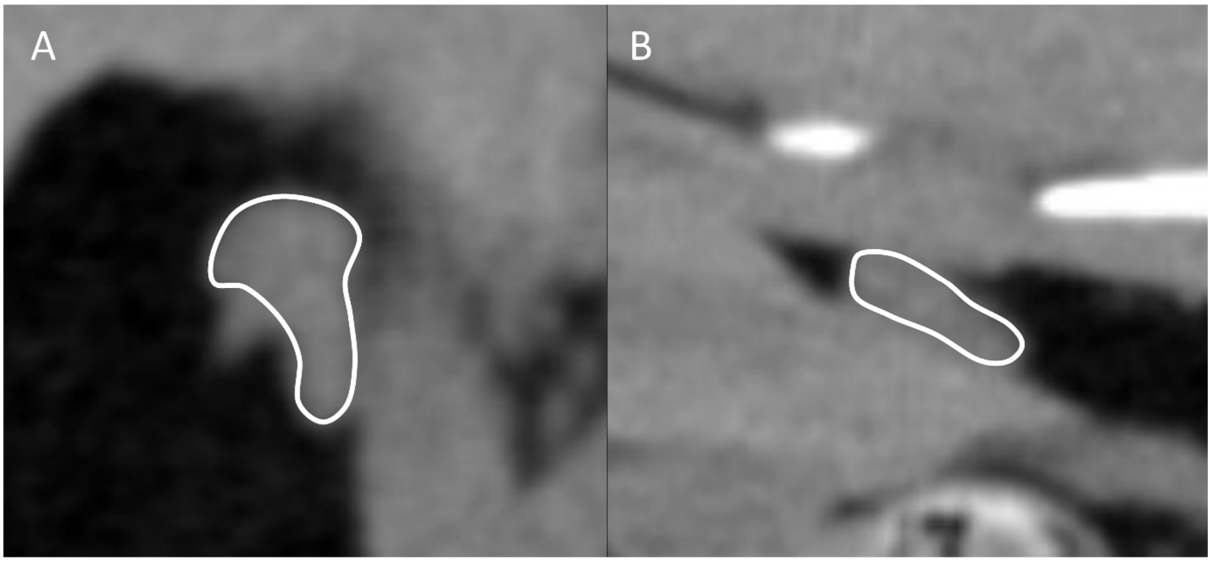

Figure 2 Dorsal (A) and sagittal (B) CT images of a right arrowhead shaped adrenal gland displayed in soft tissue window. The arrowhead shape can be clearly seen in the dorsal plane in contrast to the sagittal plane where the cross-sectional area is oval and does not correspond to the three-dimensional shape of the adrenal gland.

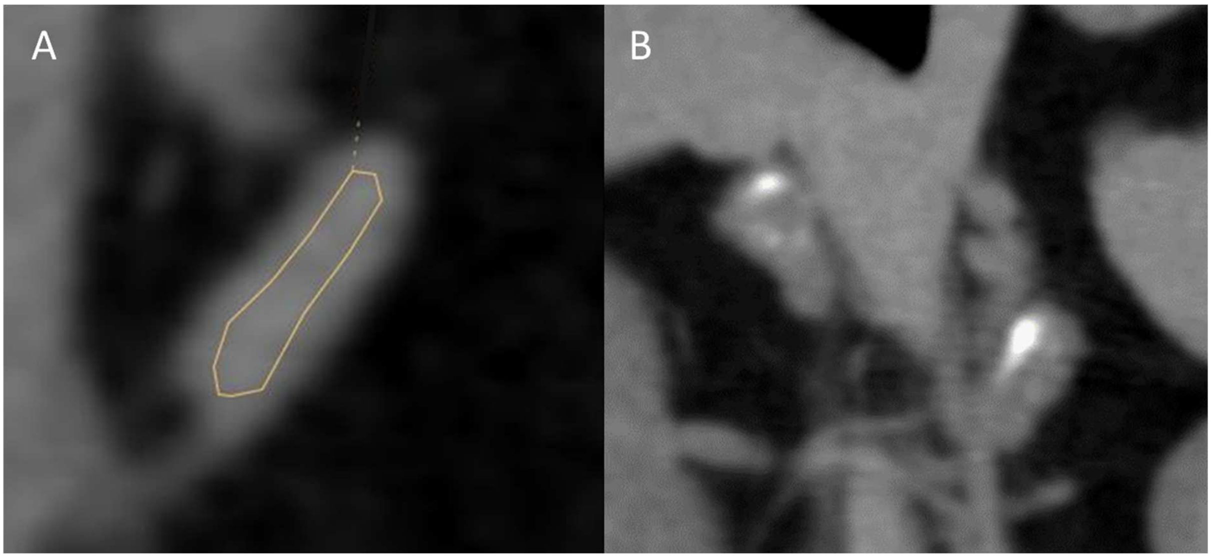

Figure 3 Dorsal CT images of the left adrenal gland (A) and both adrenal glands (B) of cats from NAD-group displayed in soft tissue window. (A) The ROI outline is traversed by hand over the cross-sectional area of the adrenal, excluding vessels and gland borders to avoid partial volume effects and exclude periadrenal fat. The software calculates automatically attenuation values of the ROI in HU. (B) Bilateral mineralization of the adrenal glands.

Intra- and inter-observer agreement

To assess intra-observer agreement, 30 randomly selected anonymized cats from PAD-group were re-evaluated by the same radiologist following a three-month interval. A second observer, a boarded imaging diplomate (EL), evaluated the same cats once to permit inter-observer agreement assessment.

Computed tomography acquisition

The NAD-group received a standardized intravenous protocol for anaesthesia: midazolam[b] (0.2 mg/kg), butorphanol[c] (0.2 mg/kg), ketamine[d] (1–5 mg/kg), propofol[e] (2–4 mg/kg) and sevoflurane[f] (1.5–2.2 % in 100 % of O2 at 2 l/min). Scans were performed in sternal position with breath-holding technique. In addition to the region, clinically indicated by the cats non-adrenal disease, abdominal images were acquired from cranial to the diaphragm to caudal to the coxofemoral joint with 130 kVp, 80–120 mAs, a pitch of 1, a scan matrix of 512 x 512 and a slice thickness of 0.75 mm. In both groups, a 16-slice helical CT scanner[g] was used. As the PAD-group was analysed retrospectively, the protocol for general anaesthesia and scanning was not standardized. The scanned region and body position depended on the clinical indication. Acquisition settings included: algorithm- thoracic, abdominal, total-body, spinal, 110–130 kVp, 80–180 mAs, a pitch of 1, scan matrix of 512 x 512, slice thickness of 0.75 (n = 82) or 1 mm (n = 10), field of view of 59–383 mm.

Statistical analysis

Statistical analysis was performed using IBM SPSS v24 software[h]. The assumption of normal distribution was assessed using Kolmogorov-Smirnov test. Most data did not show a normal distribution. Differences between groups in age, sex, bodyweight and BCS were analysed using Mann-Whitney U tests. The Student's *t* test was applied, when distribution was normal. Spearman's correlation coefficient (r) was used to analyse the correlation between adrenal gland variables (size, attenuation, delineation grade and the presence of mineralization or masses) and age, sex, laterality, BCS and body weight of cats. The Pearson correlation coefficient (r) and paired samples t-test were performed to test intra- and inter-observer agreements. For all statistical analyses $P<0.05$ was considered significant.

Results

Signalment, mean body weight and mean BCS of both groups are summarized in table 1. Thirty and 92 cats were included in the NAD- and PAD-groups, respectively. There was no significant difference between these groups in terms of age, sex, breed distribution, body weight and BCS.

Table 1

Overview of the signalment, body weight and BCS in cats with no evidence of adrenal disease (NAD-group) and with possible adrenal disease (PAD-group)

		NAD-group (n = 30)	PAD-group (n = 92)
Age (years)	Mean ± SD	6.7 ± 3.2	8.3 ± 4.6
Sex number of cats (%)	Entire male	1 (3.3 %)	2 (2.2 %)
	Neutered male	17 (56.7 %)	46 (50.0 %)
	Entire female	1 (3.3 %)	3 (3.3 %)
	Neutered female	11 (36.7 %)	41 (44.5 %)
Breed number of cats (%)	Domestic shorthair	20 (66.7 %)	67 (72.8 %)
	Maine coon	6 (20.0 %)	6 (6.5 %)
	British shorthair	0	6 (6.5 %)
	Other breeds*	4 (13.3 %)	13 (14.2 %)
Body weight (kg)	Mean ± SD	5.2 ± 1.6	4.9 ± 1.3
BCS (1–5)	Mean ± SD	3.1 ± 0.8	3.2 ± 0.8

*Breeds, represented by one or two cats each, are summarized under other breeds. BCS = body condition score, BCS was evaluated using five classes: thin (1), underweight (2), ideal (3), overweight (4), obese (5)[15]

The adrenal glands were visualized in all cats. Adrenal gland dimensions, shape, attenuation and the frequency of mineralization are summarized for both groups in table 2, along with comparable data of current sonographic and computed tomographic publications. Although adrenal disease was not excluded in the PAD-group, no cat had adrenal disease as an indication for CT imaging.

Table 2

Computed tomographic and ultrasound characteristics of adrenal glands in cats with non-adrenal disease, in cats with possible adrenal disease and in healthy cats

		Computed tomography				Ultrasound	
		Cats with no evidence of adrenal disease (n = 30)*	Cats with possible adrenal disease (n = 92)*	Healthy cats (n = 27)±	Healthy cats (n = 30)†	Healthy cats (n = 94)**	Chronic sick cats non endocrine disease (n = 51)**
Adrenal length Mean ± SD Min – Max (mm)	Right	11.5 ± 2.2 7–16.7	11.7 ± 2.2 6.9–17.8	11.4 ± 2.1 7.6–15.1	10.3 ± 2.4 –	10.8 ± 1.9 (6.1–17.7)	10.9 ± 2.0 (6.7–14.7)
	Left	11.8 ± 1.7 8.9–17.4	11.6 ± 2.0 7.9–18.1	11.8 ± 1.9 7.8–15.4	10.9 ± 1.7 –	10.4 ± 1.8 (5.8–14.1)	10.8 ± 2.0 (6.9–15.5)
Adrenal width Mean ± SD Min – Max (mm)	Right	6.4 ± 1.2 4.4–8.8	6.2 ± 1.3 2.6–10.7	6.6 ± 1.2 3.8–8.4	–	–	–
	Left	5.4 ± 0.8 3.8–7.1	5.7 ± 1.3 3.9–13.5	5.6 ± 1.2 3.7–9.2	–	–	–
Adrenal height Mean ± SD Min – Max (mm)	Right	4.5 ± 0.9 3.5–7.7	5.0 ± 1.3 3.2–13	4.1 ± 0.7 2.6–5.7	3.5 ± 0.8±±	3.7 ± 0.9±± (1.5–6.7)	4.0 ± 1.2±± (1.5–7.5)
	Left	4.5 ± 0.8 3.5–7.1	5.3 ± 1.2 3.0–11.3	4.6 ± 0.9 3.2–7.2	3.5 ± 0.6±±	3.8 ± 0.8±± (1.8–5.9)	4.2 ± 0.9±± (2.3–5.8)
Right adrenal shape n of adrenals (%)	Bipolar	13 (43.3 %)	27 (29.3 %)	11 (41.0%)	0	58 (62 %)	33 (65 %)
	Oval	10 (23.3 %)	39 (42.4 %)	0	30 (100.0 %)	17 (18 %)	10 (19 %)
	Arrowh.	7 (23.3 %)	25 (27.2 %)	16 (59%)	0	–	–
	Elong.	–	–	–	0	19 (20 %)	8 (16 %)
	Not det.	0	1 (1.1 %)	0	0	0	0
Left adrenal shape n of adrenals (%)	Bipolar	8 (26.7 %)	21 (22.8 %)	10 (37.0%)	0	67 (71 %)	31 (61 %)
	Oval	22 (73.3%)	60 (65.2 %)	16 (59.0%)	30 (100.0 %)	20 (21 %)	13 (25 %)
	Arrow.	0	7 (7.6 %)	1 (4%)	0	–	–
	Elong.	–	–	–	0	7 (8 %)	7 (14 %)
	Not det.	0	4 (4.3%)	0	0	0	0
CT attenuation values (HU) Mean ± SD Min – Max	Right	33.1 ± 5.0 23.5–43.8	35.3 ± 5.5 20.5–49.0	35.3 ± 9.6 14.8–64.4	32.1 ± 11.0	–	–
	Left	32.5 ± 5.3 22.7–41.4	34.2 ± 5.3 20.7–46.7	35.5 ± 1.4 20.8–50.9	33.0 ± 12.8	–	–
Mineralization n (% per side)	Right	3 (10.0%)	10 (10.9%)	0	1 (3.3%)	–	–
	Left	4 (13.3%)	6 (6.5%)	1 (4.0%)	0	–	–

*Data from the present study, ± Mallol et al. 2019, † Phoomvuthisarn et al. 2019, ** Combes et al. 2013, ±± Cranial adrenal height was measured, Arrow. = arrowhead, Elong. = elongated, Not det. = not determined, HU = Hounsfield Units, – = not applicable in this study

The maximal dimensions and ranges were larger for the PAD-group, however only the mean right adrenal height (P = 0.01) and the mean left adrenal width (P = 0.01) achieved significance when compared with the NAD-group. In the PAD-group, dimensions of some adrenal glands were several mm above the maximum of the NAD-group. No masses, pronounced asymmetries, or abnormal shapes were detectable in any of the adrenal glands. Adrenal gland height was significantly larger on the left side in both groups, when compared to the right side (NAD-group: P = 0.02, PAD-group: P = 0.01). Right adrenal gland width was significantly wider than the left side in the NAD-group (P = 0.01).

Delineation of the left adrenal gland did not diverge significantly (P = 0.27) between the NAD-group (mean 1.2 ± 0.8) and the PAD-group (mean 1.4 ± 0.7). In contrast, the grade of delineation of the right adrenal gland was significantly (P = 0.049) better in NAD-group (mean 1.4 ± 0.6) compared with the PAD-group (mean 1.7 ± 0.6). Subjectively the left adrenal gland was easier to delineate than the right in both groups, however difference in delineation only achieved statistical significance in the PAD-group (P = 0.04).

Adrenal glands without mineralizations exhibited homogenous parenchyma. There was no layering, consistent with corticomedullary differentiation, detectable. Adrenal glands were positioned craniomedial to the ipsilateral kidney. In both groups the right adrenal gland was typically bordering the liver and the Vena cava caudalis (VCcd) and positioned dorsolateral or lateral to the VCcd and ventrolateral to the Aorta abdominalis (Aabd). The left adrenal gland was regularly bordering the VCcd, less often the Arteria mesenterica cranialis and seldom the Vena renalis or Aabd or other surrounding vessels or organs. It was positioned lateral or dorsolateral to the VCcd, frequently ventrolateral, seldom ventral to the Aabd.

Adrenal gland shape did not differ significantly between groups and was best recognized in the dorsal plane. The sagittal plane was misleading when evaluating the three-dimensional adrenal gland shape, especially regarding the arrowhead shape (Figure 2A, B). In both groups, a bipolar or oval shape was most frequently observed. The arrowhead shape was least frequently observed and identified in 7 (23.3 %) and 25 (27.2 %) right adrenal glands in the NAD-group and the PAD-group, respectively. In the NAD-group none of the left adrenal glands were of arrowhead shape, but in the PAD-group 7 (7.6 %) adrenal glands were.

Mean adrenal gland attenuation did not differ significantly between left and right within groups and between groups. The range of attenuation in the PAD-group was wider, but cats in the PAD-group only mildly exceeded the range of the NAD-group (≤ 13.7 HU). The frequency of mineralization did not differ significantly between groups or lateralisations (NAD-group right: 3 [10 %], left: 4 [13.3 %], PAD-group right: 10 [10.9 %], left: 6 [6.5 %]).

Intra-observer agreement of adrenal size measurements and attenuation was good to excellent. It was $r = 0.92$ for length, $r = 0.83$ for width, $r = 0.84$ for height and $r = 0.81$ for attenuation with $P \leq 0.01$ for all results. Inter-observer agreement was moderate to good. It was $r = 0.88$ for length, $r = 0.80$ for width, $r = 0.72$ for height and $r = 0.54$ for attenuation with $P \leq 0.01$ for these results. There were no significant differences between means of the adrenal gland dimensions within and between observers.

Few associations were identified between adrenal gland CT parameters and signalment. Right adrenal gland height in the NAD-group was the only aCTc that correlated ($r = 0.51$, $P = 0.01$) with cats' age. Left adrenal gland delineation in the PAD-group exhibited mild negative correlation ($r = –0.31$, $P = 0.01$) with BCS (therefore improving with a rising BCS). Delineation grade did not correlate with body positioning. There was no statistically significant association between adrenal gland size, attenuation, delineation grade, presence of mineralization or masses and age, sex, BCS and body weight.

Discussion

To the authors' knowledge this is the first study that investigated the presence of adrenal gland structural changes in a group of cats using CT. Adrenal masses were not identified in any cat under investigation. This is of interest, as the prevalence of incidentally identified adrenal masses, so called "incidentalomas" was 3–7 % in human and 4–9 % in canine studies, respectively.[11,12,14,17,18] The fact that no adrenal mass was found in 92 cats is a significant contrast to human and canine studies, but in line with the reported incidence of 0.03 % for feline adrenal neoplasia.[10]

Radiological findings indicating the presence of adrenal gland neoplasia include increased size, heterogeneity, irregular borders and vascular invasion whether identified in ultrasonography, CT or MRI.[10] Although the mean right adrenal gland height and left adrenal gland width were higher and the range of dimensions was larger in the cats with possible adrenal disease compared with cats with likely normal adrenal glands, adrenal gland masses were not identified. It is important to note that, as the measurements and characteristics of normal and diseased adrenal glands overlap, neoplasia or bilateral hyperplasia can remain occult on ultrasound and CT.[19,20] Different body positioning can lead to differing adrenal size measurements and this could have contributed to the wider size range in the PAD-group.[21] The absence of adrenal masses in this selected group of cats suggests that in contrast to other species, adrenal masses rarely occur in cats. Their identification should prompt the clinician to perform further investigations to clarify the clinical importance.

Both groups consisted of cats undergoing CT for reasons unrelated to adrenal disease. The NAD-group was recruited prospectively and screened for clinical signs and laboratory changes associated with adrenal disease. Thus, it is rather unlikely that adrenal disease was present within this group. Furthermore, mean adrenal gland size and standard deviation of NAD-group were consistent with a recent study in healthy cats.[5] The fact that slightly lower dimensions were reported by Phoomvuthisarn and others could be the consequence of including juvenile cats in that study.[6] Consistent with a recent healthy cat study, the right adrenal in the NAD-group was significantly wider than the left.[5] We hypothesize this is due to the arrowhead shape that predominantly occurred on the right side. Ultrasonographic studies do not report this difference in widths, probably due to the differing manner of measurement.[4]

Not unexpected, adrenal lesions were very rare in the PAD-group and comparable to changes found in the NAD-group. This can be explained by overall low incidence of feline adrenal disease including adrenal masses in cats and is consistent with recent ultrasonographic studies, where aCTc of healthy cats were very similar to that of animals with non-endocrine diseases.[4,10,22] Nevertheless, the likelihood to identify adrenal lesions was higher in the PAD-group, because this group was recruited retrospectively without prior screening for adrenal disease. In the NAD-group cats with diseases that could influence adrenal function or mineralization were excluded. Nevertheless, it is possible that non-adrenal diseases could affect adrenal size or other aCTc. This might have influenced the differences found between both groups.

Generally, the reported ultrasonographic dimensions are smaller than our findings.[1,2,4,22] This is not surprising as measurements of abdominal organs in CT are regularly higher in direct comparison to ultrasound.[23] We hypothesize that the reason for this is that it is easier to recognize the ideal plane for maximal dimension in multiplanar reconstructions of CT, unlike ultrasound, where animal conformation and bowel gas can hinder evaluation.

The main differences between the present and earlier studies include the adrenal gland shape and the prevalence of mineralization. One recent healthy cat study reported no oval shaped right adrenal glands, conversely another study reported all adrenal glands to be oval in shape.[5,6] Consistent with the first study involving healthy cats, the arrowhead shape was almost entirely limited to the right adrenal gland.[5] This contrasts with ultrasound findings, where a similar shape distribution (elongated, oval, bilobed) between both adrenal glands was reported.[1,2] In ultrasonographic studies, the arrowhead shape was not reported, consequently this is another reason why the frequency of shapes/conformation differed to our groups.[1,2,4] Multiplanar reconstruction may result in a differing assessment of shape than ultrasonographic evaluation

(Figure 2A, B). Sonographic assessment of shape in sagittal plane can be influenced by obliqueness.[3] In contrast to CT studies involving healthy cats, mineralization was markedly more frequent in our study, consistent with ultrasound where hyperechoic foci (suspicious for mineralizations) occurred in 20 % of diseased cats, but only in 9 % of healthy cats.[4] The adrenal glands of the NAD-group had mineralizations, but there was no evidence of adrenal gland disease. This is consistent with histopathological studies that identified adrenal mineralization as mainly dystrophic, seldom related to adrenalitis and not indicative of adrenal neoplasia.[13,24] When adrenals glands with mineralizations and as a consequence higher attenuation were excluded, adrenal gland attenuation of our groups was consistent with studies involving healthy cats.[5,6]

In this study the associations of aCTc with signalment and adrenal gland position largely mirrored previous publications. In both groups, the position of the adrenals relative to the kidneys, VCcd and Aabd was consistent with the previously published literature.[6,25] In our study the left adrenal gland was bordering the VCcd with a higher frequency than the Aabd, which contrasts anatomical literature about dogs and cats and to our knowledge, has not been reported for normal feline adrenal glands in CT studies.[26,27] In agreement with several studies, body weight, BCS and sex did not influence adrenal gland size and attenuation.[2,4,5,22] Unlike an earlier CT study including healthy cats, wider adrenal glands were not identified in male cats in our populations.[5] Regarding adrenal gland size, the sole moderate positive correlation was right adrenal gland height and age. This contrasts with ultrasound and CT studies where a mild reduction of adrenal gland length with increasing age, or no association with adrenal gland size was reported.[3,5] Due to the scarcity of intact male and female cats, the impact of neutering was impossible to assess.

This study has several limitations. The main drawback is the lack of a suitable gold standard like histopathological analysis to prove normal adrenal structure. It is thus possible, that we unintentionally included cats with various adrenal diseases. The NAD-group was screened prospectively to the best of our ability with clinical and laboratory examinations. It is also possible that subtle structural changes within the adrenal parenchyma were not identified in CT in the PAD-group. Contrast enhanced CT may have increased the diagnostic value of this study. Given its retrospective nature, it was not possible to standardize CT studies for the PAD-group. The variable body positioning during the CT scan and the few cases with slightly thicker slices (1 mm instead of 0.75 mm) may have influenced the measurements of the aCTc. However, as partial averaging decreases with thinner slice thickness, we believe the small difference of 0.25 mm had minimal effect .[28] Whilst the tube settings varied in the PAD-group (80–180 mAs), the studies were of diagnostic quality and thus difference in current was unlikely to account for any differences identified. The number of cats in the PAD-group (n = 92) was considerable, but due to the low prevalence of feline adrenal masses and the applied selection criteria, higher numbers and a representative population are needed to assess the general prevalence of feline adrenal masses in CT reliably. The increasing usage of CT in veterinary medicine will likely facilitate the adequate study number for comparable studies in the future.

Conclusion

Adrenal gland size of cats with non-adrenal disease but no evidence of adrenal disease is similar to that of healthy cats when measured in CT. In contrast, adrenal gland shapes and their frequency differed partially and adrenal gland mineralization was markedly more frequent than previously reported in healthy cats. Otherwise characteristics and correlations were largely similar. The fact that no adrenal gland mass was detected in both study groups might indicate that adrenal masses overall are rare in cats with no symptoms indicating adrenal disease. The identification of a so called adrenal "incidentaloma" should prompt further investigation to clarify the clinical importance. The authors acknowledge the small number in the study population and that a larger study is needed to confirm the frequency and the character of structural adrenal changes in a larger feline population. Ideally, these should be supplemented by histopathological analyses.

Footnotes

a	JiveX Diagnostic Advanced 5.0.4.4, VISUS Health IT GmbH, Bochum, Germany
b	Dormicum, Roche Pharma, Grenzach-Wyhlen, Germany
c	Alvegesic, Alvetra und Werfft, Vienna, Austria
d	Ketamidor, Richter Pharma, Wels, Austria
e	Propofol Fresenius, Fresenius Kabi Austria, Graz, Austria
f	Sevorane, AbbVie Deutschland, Wiesbaden, Germany
g	Siemens Somatom Emotion, Siemens Healthcare AG, Zürich, Switzerland
h	IBM SPSS v24 software, IBM Corp., Armonk, New York

Abbrevations

Aabd	Aorta abdominalis
aCTc	Adrenal computed tomography characteristics
Arrow.	Arrowhead
BCS	Body Condition Score
Elong.	Elongated
HU	Hounsfield Units
NAD-Group	Non-Adrenal Disease Group
Not. Det.	Not Determined
PAD-Group	Possible Adrenal Disease Group
r	Pearson Correlation Coefficient
ROI	Region of Interest
VCcd	Vena cava caudalis

References

1 Cartee RE, Bodner STF, Gray BW. Ultrasound examination of the feline adrenal gland. *J Diagn Med Sonogr* 1993;9:327–30.

2 Zimmer C, Hoerauf A, Reusch C. Ultrasonographic examination of the adrenal gland and evaluation of the hypophyseal–adrenal axis in 20 cats. *J Small Anim Pract* 2000;41:156–60.

3 Combes A, Vandermeulen E, Duchateau L, et al. Ultrasonographic measurements of adrenal glands in cats with hyperthyroidism. *Vet Radiol Ultrasound* 2012;2:210–16.

4 Combes A, Pey P, Paepe D, et al. Ultrasonographic appearance of adrenal glands in healthy and sick cats. *J Feline Med Surg* 2013;6:445–57.

5 Mallol C, Altuzarra R, Espada Y, et al. CT characterisation of feline adrenal glands. *J Feline Med Surg* 2019;4:285–91.

6 Phoomvuthisarn P, Komin K, Choisunirachon N. Comparative ultrasonographic and computed tomographic images of the adrenal glands of healthy cats. *Thai J Vet Med* 2018;4:689–98.

7 Rijnberk A, Voorhout G, Kooistra HS, et al. Endocrinology: Hyperaldosteronism in a cat with metastasised adrenocortical tumour. *Vet Q* 2001;1:38–43.

8 Leshinsky J, Beatty JA, Fawcett A, et al. Aldosterone and progesterone–secreting adrenocortical adenocarcinoma in a cat with a concurrent meningioma. *JFMS Open Rep* 2016;1:1–7.

9 Kirkwood N, Boland L, Brunel L, et al. Acute adrenal haemorrhage in two cats with aldosterone-secreting adenocarcinomas. *JFMS Open Rep* 2019;1:1–5.

10 Myers NC. Adrenal incidentalomas. *Vet Clin North Am Small Anim Pract* 1997;2:381–99.

11 Bovio S, Cataldi A, Reimondo G, et al. Prevalence of adrenal incidentaloma in a contemporary computerized tomography series. *J Endocrinol Invest* 2006;4:298–302.

12 Choyke PL. ACR Appropriateness criteria on incidentally discovered adrenal mass. *J Am Coll Radiol* 2006;3:498–504.

13 Herbach N, Wiele K, Konietschke U, et al. Pathologic alterations of canine and feline adrenal glands. *J Pathol* 2016;6:140–53.

14 Mayo–Smith WW, Song JH, Boland GL, et al. Management of incidental adrenal masses: a white paper of the ACR incidental findings committee. *J Am Coll Radiol* 2017;14:1038–44.

15 Shoveller AK, DiGennaro J, Lanman C, et al. Trained vs untrained evaluator assessment of body condition score as a predictor of percent body fat in adult cats. *J Feline Med Surg* 2014;12:957–65.

16 Acierno MJ, Brown S, Coleman AE, et al. ACVIM consensus statement: guidelines for the identification, evaluation, and management of systemic hypertension in dogs and cats. *J Vet Intern Med* 2018;32:1803–22.
17 Cook AK, Spaulding KA, Edwards JF. Clinical findings in dogs with incidental adrenal gland lesions determined by ultrasonography: 151 cases (2007–2010). *J Am Vet Med Assoc* 2014;10:1181–85.
18 Baum JI, Boston SE, Case JB. Prevalence of adrenal gland masses as incidental findings during abdominal computed tomography in dogs: 270 cases (2013–2014). *J Am Vet Med Assoc* 2016;10:1165–69.
19 Combes A, Saunders JH. Ultrasonographic examination of the feline adrenal glands: A review. *Rev Vét Clin* 2014;49:1–12.
20 Elsayes KM, Emad–Eldin S, Morani AC, et al. Practical approach to adrenal imaging. *Radiol Clin N Am* 2017;2:279–301.
21 Vali Y, Villamonte–Chevalier A, Broeckx BJ, et al. The effect of patient positioning on adrenal gland linear measurements estimated from computed tomographic images in healthy beagle dogs. *Domest Anim Endocrinol* 2020;72:1–7.
22 Zatelli A, D'Ippolito P, Fiore I, et al. Ultrasonographic evaluation of the size of the adrenal glands of 24 diseased cats without endocrinopathies. *Vet Rec* 2007;19:658–60.
23 Groell R, Machan L, Schaffler GJ, et al. Morphometric measurement of abdominal organs. *Acta Radiol* 1997;6:982–85.
24 Hoenig M. Feline hyperadrenocorticism – where are we now? *J Feline Med Surg* 2002;4:171–74.
25 Barthez PY, Nyland TG, Feldman EC. Ultrasonography of the adrenal glands in the dog, cat, and ferret. *Vet Clin North Am Small Anim Pract* 1998;4:869–85.
26 Koenig HE, ed. Endokrine Druesen. In: Anatomie der Katze mit Hinweisen fuer die tieraerztliche Praxis. Stuttgart: Gustav Fischer Verlag, 1992: 170–73.
27 Nickel R, Schummer A, Seiferle E, eds. Endokrine Druesen. In: Lehrbuch der Anatomie der Haustiere Band 4 - Nervensystem, Sinnesorgane, Endokrine Druesen. 4th ed. Stuttgart: Parey Verlag, 2004: 473–501.
28 Schwarz T, O'Brien R. Chapter 2: CT Acquisition Principles. In: Schwarz T, Saunders J, eds. Veterinary Computed Tomography. Chichester: Wiley, 2011: 9–28.

5 Discussion

This chapter is complementary to the discussion in the publication. Within the publication the prevalence of incidentally identified adrenal masses, adrenal neoplasia, adrenal characteristics (size, shape, attenuation, laterality, position), adrenal mineralization and associations between aCTc and patient variables were discussed and compared to current literature. Additionally, the limitations of the study were addressed. The intra- and inter-observer agreement was not included in the discussion of the publication and therefore will be discussed in this chapter.

In agreement with CT measurements of other studies in dogs and cats intra- and inter-observer agreement of adrenal size was the best for adrenal length (Mallol 2019, Perfetti 2019) and was still good for width and height. The varying shape of the adrenal glands and the difficulty to determine the exact dorsoventral or mediolateral axis of this small organ likely reduced reproducibility and repeatability for adrenal width and height in comparison to length. This is in contrast to sonographic studies that assessed the highest intra- and inter-observer variability for adrenal length. In ultrasonography the height of the caudal adrenal pole in dogs and the height of the cranial and caudal pole in cats had the best intra- and inter-observer variability and therefore is the most reliable sonographic measurement of adrenal size (Barberet 2010, Combes 2014b).

The set up and parameter of CT acquisition of this study were similar to that of Mallol et al. 2019, which allows a good comparison of inter-observer agreement. Both studies used a 16–slice helical CT scanner, a slice thickness of 0.75–1 mm respectively 0.65 mm, and size and attenuation of feline adrenal glands were measured. Inter-observer agreement for the current study (r = Pearson correlation coefficient) and Mallol et. al. 2019 (ICC = intraclass correlation coefficient) was the same and excellent for length r = 0.88, ICC = 0.88, differed for width with r = 0.8, ICC = 0.5, for height r = 0.72, ICC = 0.6 and attenuation r = 0.54, ICC = 0.25. The largely better inter-observer agreement in this study could have been a result of combined training session of both observers before the study. In this study, the patients that were used to test intra- and inter-observer agreement were from the PAD-group and CT studies were therefore not standardised. This may have reduced the inter-observer agreement. In both studies adrenal attenuation had the lowest inter-observer agreement. In contrast to the linear measurement of an adrenal size parameter, the possibilities of selecting an area (size, position) for the measurement of adrenal attenuation are multiple. We suspect this could be another reason for the low inter-observer agreement. A high intra- and inter-observer agreement is especially important when small organs like adrenal glands are measured. We therefore advocate implementing special training of observers before measuring. Based on the result of our study the adrenal size (length, width, height) measurement in CT is reliable. Adrenal length measured in CT is the most reliable parameter of adrenal size in cats.

6 Conclusion

CT measurements of adrenal size of cats with non-adrenal disease but no evidence of adrenal disease were similar to that of healthy cats. However, they did differ regarding the frequency of adrenal mineralization. Adrenal mineralization was described markedly less frequently in healthy cats and the frequency of shapes between these groups also differed partially. Other adrenal characteristics and associations were largely similar. Adrenal length had the most reliable intra- and inter-observer agreement of adrenal size parameters. In 92 cats with possible adrenal disease, no adrenal mass was detected with CT. In contrast with humans and dogs, incidental adrenal masses appear to be very rare in cats. To confirm these results the frequency and the character of structural adrenal changes in a larger feline population, a larger study population in future studies is necessary. Ideally, these should be supplemented by histopathological analyses. In case of identification of an adrenal mass further diagnostic work up should be conducted to determine clinical relevance.

7 Ethical approval

All procedures were approved by the institutional ethics and animal welfare committee of the University of Veterinary Medicine Vienna in accordance with good scientific practice guidelines and national legislation (ETK-09/07/2018).

8 Zusammenfassung

Zielsetzung

Die Ziele der Studie waren die Beschreibung der computertomographischen Charakteristika der Nebennieren (CTCN) von Katzen, welche frei von Hinweisen auf Nebennierenerkrankungen waren, aber aufgrund von nicht-adrenalen Krankheiten einer Computertomographie (CT) unterzogen wurden (Gruppe NAK). Ein weiteres Ziel war das Auftreten von adrenalen Massen und anderen morphologische Abweichungen der CTCN in einer Gruppe von Katzen mit möglichen adrenalen Krankheiten zu beschreiben (Gruppe MAK).

Methode

Die Gruppe NAK umfasste 30 prospektiv selektierte Katzen, bei denen ein abdominales CT durchgeführt wurde und deren Anamnesen, sowie klinischen Untersuchungen und Blut-chemischen Analysen keinen Hinweis auf Nebennierenerkrankungen ergaben. Für die Gruppe MAK wurde das Archiv auf CT-Untersuchungen von erkrankten Katzen mit möglichen zusätzlichen Nebennierenerkrankungen durchsucht. Die CTCN (Größe, Form, Dichte, Position, Mineralisation) wurden beurteilt und mögliche Zusammenhänge zu Patientenparametern (Alter, Geschlecht, Seitenunterschiede, Ernährungszustand, Körpermasse) berechnet. Die Resultate wurden mit Parametern von gesunden Katzen aus aktueller Literatur verglichen. Bei der Gruppe MAK wurde das Auftreten von morphologischen adrenalen Veränderungen und Massen untersucht, wofür die Gruppe NAK als Referenz diente.

Ergebnisse

Die Gruppe NAK zeigte ähnliche Zusammenhänge der Parameter und Eigenschaften der CTCN wie Länge (rechts: 11,5 ± 2,2 mm, links: 11,8 ± 1,7 mm), Breite (rechts: 6,4 ± 1,2 mm, links: 5,4 ± 0,8 mm), Höhe (rechts: 4,5 ± 0,9 mm, links: 4,5 ± 0,8 mm), Dichte (rechts: 33,1 ± 5,0 HU, links: 32,5 ± 5,3 HU) und Position, jedoch deutlich mehr Mineralisationen (rechts: 10%, links 13,3%) als bei aktuellen Studien über gesunde Katzen bekannt ist. Die Nebennierenformen (bohnenförmig, oval, keilförmig) und ihre anteilige Verteilung unterschied sich teils zu anderen Studien. Keine der 92 Katzen der Gruppe MAK zeigte eine Nebennierenmasse.

Schlussfolgerungen und Relevanz

Die Daten dieser Studie dienen als Referenz für die CTCN von Katzen, welche frei von Hinweisen auf Nebennierenerkrankungen sind, aber eine nicht-adrenale Krankheit haben. Im Gegensatz zu Menschen und Hunden scheinen Katzen sehr selten Nebennierenmassen aufzuweisen.

9 Summary

Objectives

To describe adrenal computed tomography characteristics (aCTc) in cats with no evidence of adrenal disease that underwent CT for non-adrenal disease (NAD-group). To determine retrospectively the occurrence of adrenal masses and evaluate for other morphological deviations of aCTc in cats with possible concurrent adrenal disease (PAD-group).

Methods

Thirty prospectively selected cats, with no evidence of adrenal disease (based on clinical and laboratory examinations) and abdominal CT comprised the NAD-group. For the PAD-group the archive was searched for cats with possible concurrent adrenal disease that had previously been investigated using CT. ACTc (size, shape, attenuation, position, mineralization) were examined and associations with patient variables (age, sex, laterality, body condition score, and body weight) were tested. Results were compared with reported parameters of healthy cats in current literature. PAD-group was assessed for adrenal masses or other morphological deviations using NAD-group as reference.

Results

NAD-group showed similar associations of parameters and similar aCTc like length (right: 11.5 ± 2.2 mm, left: 11.8 ± 1.7 mm), width (right: 6.4 ± 1.2 mm, left: 5.4 ± 0.8 mm), height (right: 4.5 ± 0.9 mm, left: 4.5 ± 0.8 mm), attenuation (right: 33.1 ± 5.0 HU, left: 32.5 ± 5.3 HU), and position, but markedly more mineralizations (right: 10%, left 13.3contrast) than reported in current literature about healthy cats. Adrenal shapes (bilobed, oval, arrowhead) and their frequency differed partially to other studies. No incidental adrenal masses were identified in the 92 cats of PAD-group and only few aCTc differed significantly when compared to NAD-group.

Conclusions and relevance

This study provides a reference of aCTc for cats with non-adrenal disease, but no evidence of adrenal disease. In contrast to humans and dogs, incidental adrenal masses seem to be very rare in cats, if detected further diagnostic work-up is recommended to clarify clinical importance.

10 Abbrevations

Aabd	Aorta abdominalis
aCTc	Adrenal computed tomography characteristics
ACTH	adrenocorticotropic hormone
ALT	Alanine aminotransferase
BCS	Body Condition Score
BUN	Blood Urea Nitrogen
CEUS	Contrast enhanced ultrasonography
CT	Computed tomography
CTCN	Computertomographische Charakteristika der Nebennieren
FIC	Feline Interstitial Cystitis
Gruppe MAK	Gruppe Mögliche Adrenale Krankheiten
Gruppe NAK	Gruppe Nicht-adrenale Krankheiten
HU	Hounsfield Unit
ICC	Intraclass Correlation Coefficient
NAD-Group	Non-Adrenal Disease Group
Not. Det.	Not Determined
PAD-Group	Possible Adrenal Disease Group
r	Pearson Correlation Coefficient
ROI	Region of Interest
UPC	Urine Protein:Creatinine Ratio
UCC	Urine Cortisol:Creatinine Ratio
VCcd	Vena cava caudalis

11 References

Acierno MJ, Brown S, Coleman AE, et al. ACVIM consensus statement: guidelines for the identification, evaluation, and management of systemic hypertension in dogs and cats. *J Vet Intern Med* 2018;32:1803–22.

Agrons MM, Jensen CT, Habra MA, et al. Adrenal cortical hyperplasia: diagnostic workup, subtypes, imaging features and mimics. *Br J Radiol* 2017;90:20170330.

Ali Z, Tariq H, Rehman U. Endothelial cysts of adrenal gland. *J Coll Physicians Surg Pak* 2019;29:16–17.

Ash RA, Harvey AM, Tasker S. Primary hyperaldosteronism in the cat: a series of 13 cases. *J Feline Med Surg* 2005;7:173–82.

Barberet V, Pey P, Duchateau L, et al. Intra- and interobserver variability of ultrasonographic measurements of the adrenal glands in healthy beagles. *Vet Radiol Ultrasound* 2010;51:656–60.

Bargellini P, Orlandi R, Dentini A, et al. Use of contrast-enhanced ultrasound in the differential diagnosis of adrenal tumors in dogs. *J Am Anim Hosp Assoc* 2016;52:132–43.

Barthez PY, Nyland TG, Feldman EC. Ultrasonographic evaluation of the adrenal glands in dogs. *J Am Vet Med Assoc* 1995;207:1180–83.

Barthez PY, Nyland TG, Feldman EC. Ultrasonography of the adrenal glands in the dog, cat, and ferret*. Vet Clin North Am Small Anim Pract*. 1998;28:869–85.

Baum JI, Boston SE, Case JB. Prevalence of adrenal gland masses as incidental findings during abdominal computed tomography in dogs: 270 cases (2013–2014). *J Am Vet Med Assoc* 2016;10:1165–69.

Becker T, Perry R, Watson G. Regression of hypertrophic osteopathy in a cat after surgical excision of an adrenocortical carcinoma. *J Am Anim Hosp Assoc* 1999;35:499–505.

Bento PL, Center SA, Randolph JF, et al. Associations between sex, body weight, age, and ultrasonographically determined adrenal gland thickness in dogs with non-adrenal gland illness. *J Am Vet Med Assoc* 2016;6:652–60.

Besso JG, Penninck DG, Gliatto JM. Retrospective ultrasonographic evaluation of adrenal lesions in 26 dogs. *Vet Radiol Ultrasound* 1997;38:448–55.

Blake MA, Kalra MK, Sweeney AT, et al. Distinguishing benign from malignant adrenal masses: Multi-detector row CT protocol with 10-minute delay. *Radiol* 2006;238:578–85.

Blake MA, Boland GWL. Imaging adrenal dysfunction. *In: Adrenal imaging.* Totowa (NY): Humana Press; 2009a. pp 91–106.

Blake MA, Boland GWL. Adrenal imaging using computed tomography: Differentiation of adenomas and metastasis. In: Adrenal imaging. Totowa (NY): Humana Press; 2009b. pp 127–38.

Bouknani N, Bentaleb D, Belgadir H, et al. Tuberculose surrenalienne bilaterale: a propos d'un cas. *Pan Afr Med J* 2018;29:212.

Bovio S, Cataldi A, Reimondo G, et al. Prevalence of adrenal incidentaloma in a contemporary computerized tomography series. *J Endocrinol Invest* 2006;4:298–302.

Bravo EL, Gifford RW. Pheochromocytoma: diagnosis, localization and management. *New Engl J Med* 1984;311:1298–303.

Briscoe K, Barrs VR, Foster DF, et al. Hyperaldosteronism and hyperprogesteronism in a cat. *J Feline Med Surg* 2009;11:758–62.

Calsyn JDR, Green RA, Davis GJ, Reilly CM. Adrenal pheochromocytoma with contralateral adrenocortical adenoma in a cat. *J Am Anim Hosp Assoc* 2010;46:36–42.

Caoili EM, Korobkin M, Francis IR, et al. Delayed enhanced CT of lipid-poor adrenal adenomas. *AJR Am J Roentgenol* 2000;175:1411–15.

Caoili EM, Korobkin M, Francis IR, et al. Adrenal masses: Characterization with combined unenhanced and delayed enhanced CT. *Radiology* 2002;222:629–33.

Cartee RE, Bodner STF, Gray BW. Ultrasound examination of the feline adrenal gland. *J Diagn Med Sonogr* 1993;9:327–30.

Chandrasekar T, Goldberg H, Klaassen Z, et al. The who, when, and why of primary adrenal malignancies: Insights into the epidemiology of a rare clinical entity. *Cancer* 2019;125:1050–9.

Choyke PL. ACR Appropriateness criteria on incidentally discovered adrenal mass. *J Am Coll Radiol* 2006;3:498–504.

Combes A, Vandermeulen E, Duchateau L, et al. Ultrasonographic measurements of adrenal glands in cats with hyperthyroidism. *Vet Radiol Ultrasound* 2012;2:210–6.

Combes A, Pey P, Paepe D, et al. Ultrasonographic appearance of adrenal glands in healthy and sick cats. *J Feline Med Surg* 2013;6:445–57.

Combes A, Saunders JH. Ultrasonographic examination of the feline adrenal glands: A review. *Rev Vét Clin* 2014a;49:1–12.

Combes A, Stock E, Van der Vekens E, et al. Ultrasonographical examination of feline adrenal glands: intra- and inter-observer variability. *J Feline Med Surg* 2014b;16:937–42.

Cook AK, Spaulding KA, Edwards JF. Clinical findings in dogs with incidental adrenal gland lesions determined by ultrasonography: 151 cases (2007–2010). *J Am Vet Med Assoc* 2014;10:1181–85.

DeMaio DN. Review of imaging procedures in computed tomography. In: Mosby's exam review for computed tomography. 2nd ed. St. Louis (MO): Mosby Elsevier; 2011, pp 21–72.

Dietrich C, Ignee A, Barreiros A, et al. Contrast-enhanced ultrasound for imaging of adrenal masses. *Ultraschall Med* 2010;31:163–68.

Dineen R, Stewart PM, Sherlock M. Acromegaly. *Q J Med* 2017;110:411–20.

Douglass JP, Berry CR, James S. Ultrasonographic adrenal gland measurements in dogs without evidence of adrenal disease. *Vet Radiol Ultrasound* 1997;38:124–30.

Elsayes KM, Emad–Eldin S, Morani AC, et al. Practical approach to adrenal imaging. *Radiol Clin N Am* 2017;2:279–301.

Else T, Kim AC, Sabolch A, et al. Adrenocortical carcinoma. *Endocr Rev* 2014;35:282–326.

Ettinger, S.J., Feldman, E.C. Hypoadrenocorticism. In: Veterinary internal medicine diseases of the dog and cat. 7th ed. St. Louis (MO) Saunders Elsevier, 2010, pp. 1847–57.

Fassnacht M, Arlt W, Bancos I, et al. Management of adrenal incidentalomas: European society of endocrinology clinical practice guideline in collaboration with the european network for the study of adrenal tumors. *Eur J Endocrinol* 2016;175:G1–G34.

Feldman EC, Nelson RW. Chapter 4: Feline hyperthyroidism (Thyrotoxicosis). In: Canine and feline endocrinology and reproduction. 3rd ed. St. Louis (MO): Saunders Elsevier; 2004a, pp. 153–218.

Feldman EC, Nelson RW. Chapter 7: Hyperadrenocorticism in cats (Cushing's syndrome). In: Canine and feline endocrinology and reproduction. 3rd ed. St. Louis (MO): Saunders Elsevier; 2004b, pp. 358–92.

Friedrich-Rust M, Schneider G, Bohle RM, et al. Contrast-enhanced sonography of adrenal masses: differentiation of adenomas and nonadenomatous lesions. *Am J Roentgenol* 2008;191:1852–60.

Gallagher TF, Hellman L, Finkelstein J, et al. Hyperthyroidism and cortisol secretion in man. *J Clin Endocrinol Metab* 1972;34:919–27.

Gregori T, Mantis P, Benigni L, et al. Comparison of computed tomographic and pathologic findings in 17 dogs with primary adrenal neoplasia. *Vet Radiol Ultrasound* 2015;56:153–59.

Grooters AM, Biller DS, Theisen SK, et al. Ultrasonographic characteristics of the adrenal glands in dogs with pituitary-dependent hyperadrenocorticism: Comparison with normal dogs. *J Vet Intern Med* 1996;10:110–5.

Heinz-Peer G, Memarsadeghi M, Niederle B. Imaging of adrenal masses. *Curr Opin Urol* 2007;17:32–8.

Herbach N, Wiele K, Konietschke U, et al. Pathologic alterations of canine and feline adrenal glands. *J Pathol* 2016;6:140–53.

Hindman N, Israel GM. Adrenal gland and adrenal mass calcification. *Eur Radiol* 2005;15:1163–67.

Hoenig M. Feline hyperadrenocorticism – where are we now? *J Feline Med Surg* 2002;4:171–4.

Hoerauf A, Reusch C. Ultrasonographic evaluation of the adrenal glands in six dogs with hypoadrenocorticism. *J Am Anim Hosp Assoc* 1999;35:214–8.

Hoffman EP, Barr ML, Giovanni MA, et al. Lysosomal acid lipase deficiency. In: Adam MP, Ardinger HH, Pagon RA, et al. (eds) *GeneReviews (Internet).* Seattle (WA): University of Washington, 2015.

Javadi S, Djajadiningrat-Laanen SC, Kooistra HS, et al. Primary hyperaldosteronism, a mediator of progressive renal disease in cats. *Domest Anim Endocrinol* 2005;28:85–104.

Khong PL, Lam KY, Ooi CGC, et al. Mature teratomas of the adrenal gland: imaging features. *Abdom Imag* 2002;27:347–50.

Kirkwood N, Boland L, Brunel L, et al. Acute adrenal haemorrhage in two cats with aldosterone-secreting adenocarcinomas. *JFMS Open Rep* 2019;1:1–5.

Kim KM. Apoptosis and calcification. *Scanning Microsc* 1995; 9:1137–78.

Kloos RT, Gross MD, Francis IR, et al. Incidentally discovered adrenal masses. *Endocr Rev* 1995;16:460–84.

Koenig HE. Endokrine Druesen. In: Anatomie der Katze mit Hinweisen fuer die tieraerztliche Praxis. Stuttgart (DE): Gustav Fischer Verlag, 1992, pp 170–3.

Koenig HE, Liebich H. Anatomie der Haustiere (eds). Anatomie der Haustiere. 7th ed. Stuttgart: Georg Thieme, 2019, pp 583–92.

Korobkin M, Francis IR. Adrenal imaging. *Semin Ultrasound CT MR* 1995;16:317–30.

Kuijten AM, Schoemaker NJ, Voorhout G. Ultrasonographic visualization of the adrenal glands of healthy ferrets and ferrets with hyperadrenocorticism. *J Am Anim Hosp Assoc* 2007;43:78–84.

Labelle P, De Cock HE. Metastatic tumors to the adrenal glands in domestic animals. Vet Pathol 2005;42:52–8.

Lam KY, Chan ACL, Lo CY. Morphological analysis of adrenal glands: A prospective analysis. *Endocr Pathol* 2001;12:33–8.

Lam KY, Lo CY. Metastatic tumours of the adrenal glands: a 30-year experience in a teaching hospital. *Clin Endocrinol* 2002;56:95–101.

Lee JE, Evans DB, Hickey RC, et al. Unknown primary cancer presenting as an adrenal mass: Frequency and implications for diagnostic evaluation of adrenal incidentalomas. *Surgery* 1998;124:1115–22.

Leshinsky J, Beatty JA, Fawcett A, et al. Aldosterone and progesterone–secreting adrenocortical adenocarcinoma in a cat with a concurrent meningioma. *JFMS Open Rep* 2016;1:1–7.

Lourenco, BN, Randall E, Seiler G, et al. Abdominal ultrasonographic findings in acromegalic cats. *J Feline Med Surg* 2015;17:698–703.

Lunn KF, Page RL. Tumors of the endocrine system. In: Withrow SJ and Vail DM (eds). Withrow and McEwen's small animal clinical oncology. 5th ed. St. Louis (MO): Saunders Elsevier, 2013, pp 504–31.

Maher ER, McNiel EA. Pheochromocytoma in dogs and cats. *Vet Clin North Am Small Anim Pract* 1997;27:359–80.

Mallol C, Altuzarra R, Espada Y, et al. CT characterisation of feline adrenal glands. *J Feline Med Surg* 2019;4:285–91.

Mansmann G, Lau J, Balk E, et al. The clinically inapparent adrenal mass: Update in diagnosis and management. *Endocr Rev* 2004;25:309–40.

Mantero F, Terzolo M, Arnaldi G, et al. A survey on adrenal incidentaloma in Italy. J *Clin Endocrinol Metab* 2000;85:637–44.

Mayo–Smith WW, Song JH, Boland GL, et al. Management of incidental adrenal masses: a white paper of the ACR incidental findings committee. *J Am Coll Radiol* 2017;14:1038–44.

Meier JM, Alavi A, Iruvuri S, et al. Assessment of age-related changes in abdominal organ structure and function with computed tomography and positron emission tomography. *Semin Nucl Med* 2007;37:154–72.

Myers NC. Adrenal incidentalomas. *Vet Clin North Am Small Anim Pract* 1997;2:381–99.

Newhouse JH, Heffess CS, Wagner BJ, et al. Large degenerated adrenal adenomas: Radiologic-pathologic correlation. *Radiology* 1999;210:385–91.

Nickel R, Schummer A, Seiferle E. Endokrine Druesen. In: Lehrbuch der Anatomie der Haustiere Band 4 - Nervensystem, Sinnesorgane, Endokrine Druesen. 4th ed. Stuttgart (DE): Parey Verlag, 2004, pp 473–501.

O'Brien RT, Paul-Murphy J, Dubielzig RR. Ultrasonography of adrenal glands in normal ferrets. *Vet Radiol Ultrasound* 1996;37:445–8.

Pappa T, Papanastasiou L, Koutmos S, et al. Pattern of adrenal morphology and function in patients with acromegaly. *Eur J Clin Invest* 2012;42:275–81.

Pagani E, Tursi M, Lorenzi C, et al. Ultrasonographic features of adrenal gland lesions in dogs can aid in diagnosis. *BMC Vet Res* 2016;12:267:1–9.

Park BK, Kim CK, Kim B, et al. Comparison of delayed enhanced CT and chemical shift MR for evaluating hyperattenuating incidental adrenal masses. *Radiol* 2007;243:760–5.

Penninck D, Feldman E, Nyland T. Radiographic features of canine hyperadrenocorticism caused by autonomously functioning adrenocortical tumors: 23 cases (1978–1986). *J Am Vet Med Assoc* 1988;192:1604–8.

Penninck D, dAnjou MA. Chapter 12: Adrenal Glands. In: Penninck D, dAnjou MA (eds). Atlas of small animal ultrasonography. 2nd ed. Oxford (UK): Wiley Blackwell; 2015, pp 387–401.

Perfetti S, Diana A, Baron Toaldo M, et al. Intra- and interobserver variability of multidetector-row computed tomgraphic measurements of the adrenal glands in large breed dogs. Proceedings of the European Veterinary Diagnostic Imaging Meeting, 2019 Aug 21–24; Basel, p 19.

Peterson ME, Greco DS, Orth DN. Primary hypoadrenocorticism in ten cats. *J Vet Intern Med* 1989;3:55–8.

Pey P, Rossi F, Vignoli M, et al. Use of contrast-enhanced ultrasonography to characterize adrenal gland tumors in dogs. *Am J Vet Res* 2014;75:886–92.

Phoomvuthisarn P, Komin K, Choisunirachon N. Comparative ultrasonographic and computed tomographic images of the adrenal glands of healthy cats. *Thai J Vet Med* 2018;4:689–698.

Porntharukchareon T, Khahakaew S, Sriprasart T, et al. Bilateral adrenal histoplasmosis. *Balkan Med J* 2019;36:359–60.

Rha SE, Byun JY, Jung SE, et al. Neurogenic tumors in the abdomen: tumor types and imaging characteristics. *Radiographics* 2003;23:29–43.

Rofsky NM, Bosniak MA, Megibow AJ, et al. Adrenal myelolipomas: CT appearance with tiny amounts of fat and punctate calcification. *Urol Radiol* 1989;11:148–52.

Rijnberk A, Voorhout G, Kooistra HS, et al. Endocrinology: Hyperaldosteronism in a cat with metastasised adrenocortical tumour. *Vet Q* 2001;1:38–43.

Rossmeisl JH Jr, Scott-Moncrieff J, Siems J, et al. Hyperadrenocorticism and hyperprogesteronemia in a cat with an adrenocortical adenocarcinoma. *J Am Anim Hosp Assoc* 2000;36:512–7.

Russell RGG, Caswell AM, Hearn PR, et al. Calcium in mineralized tissues and pathological calcification. *Br Med Bull* 1986;42:435–46.

Schuenke M, Schulte E, Schumacher U. Kapitel 4: Organe des Harnsystems und ihre Leitungsbahnen. In: Schuenke M, Schulte E, Schumacher U, (eds). Prometheus Innere Organe. 5th ed. Stuttgart: Georg Thieme, 2018, pp 290–317.

Schwarz T, O'Brien R. Chapter 34: Adrenal Glands. In: Schwarz T, Saunders J (eds) Veterinary Computed Tomography. Chichester (UK): Wiley, 2011, pp 351–6.

Slapa RZ, Jakubowski WS, Dobruch-Sobczak K, et al. Standards of ultrasound imaging of the adrenal glands. *J Ultrason* 2015;15:377–87.

Song JH, Grand DJ, Beland MD, et al. Morphologic features of 211 adrenal masses at initial contrast-enhanced CT: Can we differentiate benign from malignant lesions using imaging features alone? *Am J Roentgenol* 2013;201:1248–53.

Stieger-Vanegas SM, Frank PM. Chapter 39: Peritoneal Space. In: Thrall DE (ed). Textbook of veterinary diagnostic radiology. 7th ed. St. Louis (MO): Saunders Elsevier; 2018, pp 764–91.

Tidwell AS, Penninck DG, Besso JG. Imaging of adrenal gland disorders. *Vet Clin North Am Small Anim Pract* 1997;27:237–54.

Valentin SY, Cortright CC, Nelson RW, et al. Clinical findings, diagnostic test tesults, and treatment outcome in cats with spontaneous hyperadrenocorticism: 30 cases. *J Vet Intern Med* 2014,28:481–7.

Wang LJ, Wong YC, Chen CJ, et al. Imaging spectrum of adrenal pseudocysts on CT. *Eur Radiol* 2003;13:531–5.

Wang X, Jin ZY, Xue HD, et al. Evaluation of normal adrenal gland volume by 64-slice CT. *Chin Med Sci J* 2012;27:220–4.

Watson PJ, Herrtage ME. Hyperadrenocorticism in six cats. *J Small Anim Pract* 1998;39:175–84.

Westropp JL, Welk KA, Buffington CA. Small adrenal glands in cats with feline interstitial cystitis. *J Urol* 2003;170:2494–7.

Woolcock AD, Ward C. Successful treatment of a cat with primary hypoadrenocorticism and severe hyponatremia with desoxycorticosterone pivalate (DOCP). *Can Vet J* 2015;56:1158–60.

Yoshida O, Kutara K, Seki M, et al. Preoperative differential diagnosis of canine adrenal tumors using triple-phase helical computed tomography. *Vet Surg* 2016;45:427–35.

Zatelli A, D'Ippolito P, Fiore I, et al. Ultrasonographic evaluation of the size of the adrenal glands of 24 diseased cats without endocrinopathies. *Vet Rec* 2007;19:658–60.

Zimmer C, Hoerauf A, Reusch C. Ultrasonographic examination of the adrenal gland and evaluation of the hypophyseal–adrenal axis in 20 cats. *J Small Anim Pract* 2000;41:156–60.

12 Acknowledgement

I would like to express my gratitude to Univ. Prof. Dr. med. habil. Eberhard Ludewig, Dipl. ECVDI, who gave me the opportunity to conduct this study and to achieve a doctorate in veterinary medicine. As my supervisor, he had a strong personal motivation, dedication and perseverance which promoted a successful publication and my graduation. In addition, I want to express my thankfulness to Priv. Doz. Dr. med. vet. Florian K. Zeugswetter, my second supervisor, who's critical and constructive feedback substantially improved the quality of my study and the publication. The completion of this project would also not have been possible without the very pleasant and professional statistical support of Dr.rer.nat. Alexander Tichy. I also want to thank MVB DVMS Conor Rowan, Dipl. ECVDI, MRCVS, who not only alleviated my work by his committed moral and lingual support, but also helped me to shorten the text, while keeping the focus on the content. Finally, I want to thank Tzt. Maria Prüllage and Bibiane Braunöder and all the other colleagues of the Department for Companion Animals and Horses, the students and the cat owners, which were involved in the study and supported my work.